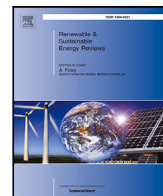




Contents lists available at ScienceDirect

Renewable and Sustainable Energy Reviews

journal homepage: www.elsevier.com/locate/rser

Infrared thermography in the built environment: A multi-scale review

Miguel Martin^a, Adrian Chong^b, Filip Biljecki^{c,d}, Clayton Miller^{b,*}^a Berkeley Education Alliance for Research in Singapore, 1 Create Way, Singapore 138602, Singapore^b Department of the Built Environment, College of Design and Engineering, National University of Singapore, 4 Architecture Drive, Singapore 117566, Singapore^c Department of Architecture, College of Design and Engineering, National University of Singapore, 4 Architecture Drive, Singapore 117566, Singapore^d Department of Real Estate, NUS Business School, National University of Singapore, 15 Kent Ridge Drive, Singapore 119245, Singapore

ARTICLE INFO

Keywords:

Infrared thermography
 Urban heat island effect
 Sustainable urban development
 Building energy performance
 Satellites
 Remote sensing
 Unmanned aerial vehicles
 Thermal imaging cameras

ABSTRACT

The paper presents a review on major contributions in infrared thermography to study the built environment at multiple scales. To elaborate the review, hundreds of studies conducted between the 1980s and 2020s were first selected based on their relevance to the scope. Afterward, the most relevant contributions were classified and chronologically sorted. From the classification, it is observed that most reviewed studies were conducted to evaluate the thermal performance of buildings or detect their defects using images collected by an infrared camera. At the same time, a considerable number of studies used thermal images obtained by a satellite to observe the urban heat island effect. Despite the important number of contributions in infrared thermography at multiple scales of the built environment, three main research gaps or opportunities can be identified in the literature. First, it would be possible to perform a more detailed analysis of urban heat fluxes using thermal images collected at multiple scales. Then, thermal images collected by a mounted or handheld infrared camera could be used to create building energy models. Finally, better visualization tools would be developed to monitor a city's energy use and improve its sustainability if thermal images were integrated into Internet-of-Things and digital twin platforms.

1. Introduction

Since the Industrial Revolution in the 19th century, a significant portion of the world population has moved from rural to urban areas. Urban areas are expected to accommodate more than 65% of the world population in 2050, and more than 85% in the most developed regions [1]. This rapid growth of the built environment has caused an augmentation of CO₂ emissions due to the building energy consumption. According to the International Energy Agency [2], 28% of the world's CO₂ emissions in 2019 are due to the energy consumed in buildings. Given this observation, considerable efforts have been made by the scientific community to better understand the built environment using different sensing technologies.

One of the most common methods to observe outdoor conditions in the built environment is to use a network of automatic weather stations [3]. Weather stations typically measure the temperature, relative humidity, pressure, wind speed and direction, solar irradiance, and rainfall, which is an important number of variables in comparison with other sensing technologies. However, one weather station only provides this set of information at a single point. As a consequence, no matter how large a network of automatic weather stations is, it will

always give information of the built environment with a limited spatial resolution.

Because of the cost and efforts that are required to observe the built environment with a satisfactory spatial resolution using automatic weather stations, or any other similar kind of sensor network, infrared thermography has gained interest within the scientific community over the years. The reason is that infrared thermography can provide images representing the surface temperature of different elements in the built environment.

Apart from giving information of the built environment with a high spatial resolution, infrared thermography can be used for many applications at multiple scales. Reviews published by Ngie et al. [4] and Almeida et al. [5] summarize applications of infrared thermography using satellites. Other reviews reported the many uses of thermal images collected by mounted or handheld infrared cameras. For instance, Balaras and Argiriou [6] described several applications of infrared thermography based on thermal images collected during a survey. This review not only focuses on the defects of the building envelope but also the failures of electrical circuits and Heating, Ventilation, and Air Conditioning (HVAC) systems that can be detected

* Corresponding author.

E-mail addresses: miguel.martin@bears-berkeley.sg (M. Martin), adrian.chong@nus.edu.sg (A. Chong), filip@nus.edu.sg (F. Biljecki), clayton@nus.edu.sg (C. Miller).

<https://doi.org/10.1016/j.rser.2022.112540>

Received 20 May 2021; Received in revised form 19 April 2022; Accepted 2 May 2022

1364-0321/© 2022 The Author(s). Published by Elsevier Ltd. This is an open access article under the CC BY license (<http://creativecommons.org/licenses/by/4.0/>).

List of abbreviations

BIM	Building Information Modelling
FLIR	Forward-Looking InfraRed
GIS	Geographic Information System
HVAC	Heating, Ventilation, and Air-Conditioning
LST	Land Surface Temperature
MODIS	Moderate Resolution Imaging Spectroradiometer
NDVI	Normalized Vegetation Difference Index
NOAA	National Oceanic and Atmospheric Administration
PV	PhotoVoltaic
RGB	Red–Green–Blue
UAV	Unmanned Aerial Vehicle
UBEM	Urban Building Energy Modelling
UHI	Urban Heat Island
UST	Urban Surface Temperature

using infrared thermography. Infrared thermography can also be applied in different manner when thermal images are collected using an Unmanned Aerial Vehicles (UAVs) as explained in the review of Rakha and Gorodetsky [7].

Instead of describing possible applications of infrared thermography at multiple scales of the built environment, most reviews explained the various methods that were used to assess the energy efficiency of a building from thermal images. These methods were classified by Fox et al. [8] concerning their measurement method, which can be qualitative or quantitative, their experimental environment, which can be indoor or outdoor, and their analysis scheme, which can be active or passive. While active infrared thermography is usually used to detect internal defects of a material or building layer using an internal or external source of excitation, passive methods aim at observing the heat emitted by a surface. The review conducted by Kylili et al. [9] elaborates more on active and passive analysis schemes in infrared thermography. In addition to classification criteria of Fox et al. [8] and Kiritmat and Krejcar [10] considered the analysis type, the envelope components, the surface material, and the testing location in their review. Other reviews focused on methods used for the energy audit of buildings as Lucchi [11] or for the detection of heat losses as Nardi et al. [12].

Regardless of whether reviews considered applications or methods of infrared thermography in the built environment, their exploration of the literature is limited to a specific scale. In particular, the majority of reviews described applications or methods of infrared thermography at the building-scale, the lowest possible scale of the built environment. Few of them reported how thermal images were used to observe the built-environment at higher scales, and none at multiple scales. Consequently, a considerable knowledge gap remains on applications of infrared thermography that were performed at one specific scale of the built environment or at multiple ones. By bridging this gap, it can be shown what kind of applications can be developed in the future to better understand the built environment at multiple scales.

For this reason, a comprehensive review is introduced on infrared thermography in the built environment at multiple scales. The objectives of the review are to: (1) show applications of infrared thermography at each scale of the built environment; (2) describe these that were performed at multiple scales; and (3) indicate research opportunities. From the review, the scientific community would gather what contribution can be made using infrared thermography at a single scale or multiple ones of the built environment. Practitioners would also learn how thermal images were collected from different infrared systems, and

how they might be integrated in the future to develop support tools in urban planning.

The review is organized as follows. The early history and fundamentals of infrared thermography are described in Section 2. Section 3 describes the methodology. Results are shown and discussed in Section 4. In Section 5, several opportunities are suggested for future research on infrared thermography in the built environment. Finally, conclusions and future work are explained in Section 6.

2. Origins and principles of infrared thermography

Research in infrared thermography has a long history of more than two centuries. Fig. 1 illustrates the timeline of important contributions between the 19th and 20th century. During the 19th century, early discoveries were found by the five fathers of infrared thermography: William Herschel and his son John, Leopoldo Nobili, Macedonio Melloni, and Samuel P. Langley. Although the 19th century represents the origin of infrared thermography, it was during the 20th century that major technological advancements were made. These technologies were developed for various sectors, including the military, medicine, and building.

In the literature, it is commonly agreed that the birth of infrared thermography was in 1800, after the publication of William Herschel [8–11]. During an experiment, he observed the visible portion of the sunlight is not the only one that can increase the surface temperature of a target object [13]. Therefore, he concluded that the sunlight is certainly composed of radiation with a higher wavelength than the visible red light, influencing the etymology of infrared. The discovery of infrared radiation led to several inventions in the 19th century. One of these inventions is the thermopile of Nobili and Melloni presented in 1831 [14]. The thermopile was created initially by Leopoldo Nobili to measure temperature. Using the first prototype of the thermopile, his associate Macedonio Melloni found a way to measure radiant heat. After the invention of the thermopile, in 1840, John Herschel, son of William Herschel, produced one of the first thermograms from the sunlight [15]. The thermogram was obtained by a method called evapography, using a lens to focus the sunlight on alcohol-containing carbon particles. Samuel P. Langley invented a more advanced technique in 1880 to measure far-infrared radiation, a component of infrared radiation [16].

Inventions in the 19th century were merely preliminary prototypes leading to modern systems for the acquisition of infrared or thermal images. The first system able to acquire thermal images from a camera was invented by Kalman Tihanyi in 1929 [17]. The camera was used for nocturnal vision by the aircraft defense. Many infrared technologies were then developed in the military sector, particularly during World War II [18]. In 1959, a system called the Pyroscan was first installed to acquire thermal images for medical use at the Middlesex Hospital in London and the Royal National Hospital for Rheumatic Diseases in Bath (United Kingdom). Twenty-four years later, in 1983, the first commercial systems were created and used for various applications in infrared thermography [19].

Most acquisition systems of thermal images that have been developed since the 1980s work on the same fundamental principles [20,21]. As illustrated in Fig. 2, systems acquiring thermal images primarily consists of a sensor. The sensor receives a heat flux L_{tot} (in W/m^2), which is a combination of several radiative heat fluxes, that is:

$$L_{tot} = \tau_a \varepsilon_s L_s + \tau_a (1 - \varepsilon_s) L_b + (1 - \tau_a) L_a \quad (1)$$

where τ_a is the transmissivity of the air between the target surface and the thermal sensor, ε_s the emissivity of the target surface, L_s the longwave radiation from the target surface (in W/m^2), L_b the longwave radiation from the background (in W/m^2), and L_a the longwave radiation from the air (in W/m^2). The longwave radiation L (in W/m^2) is a portion of the infrared radiation between 7 and 14 μm [10], which can

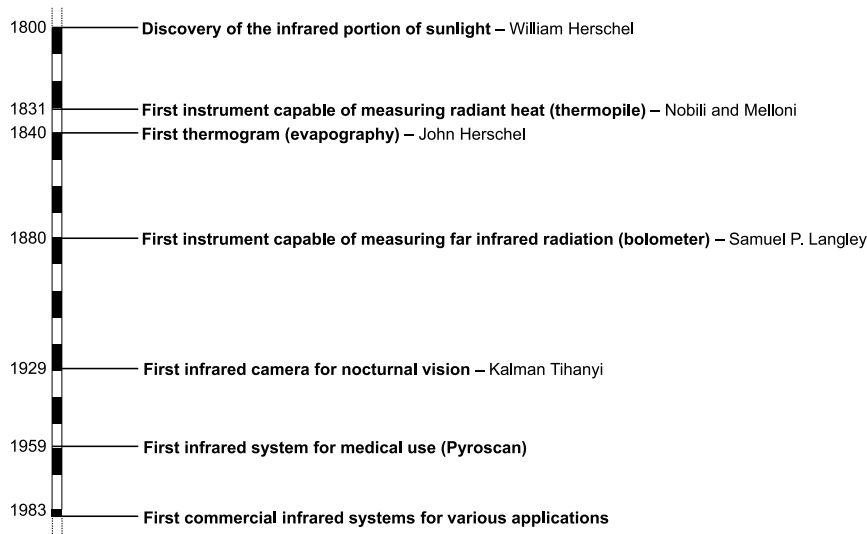


Fig. 1. History of infrared thermography between the 19th and the 20th century.

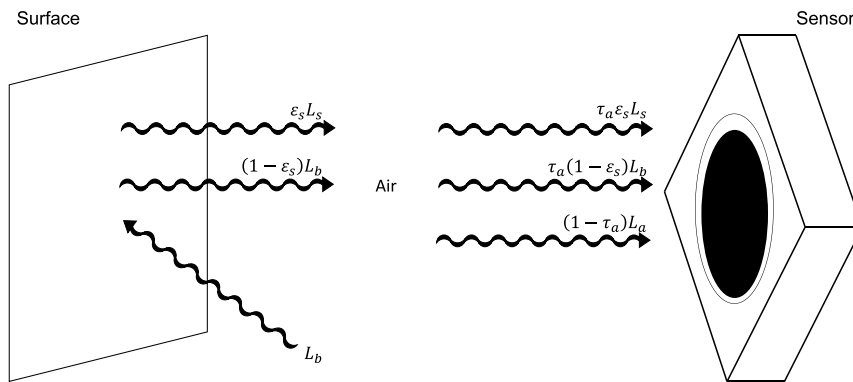


Fig. 2. Radiative heat fluxes received by a sensor to acquire thermal images.

be expressed from the surface temperature of an object T (in Kelvin) as:

$$L = \sigma T^4 \tag{2}$$

where σ is the Stefan–Boltzmann constant ($= 5.67 \cdot 10^{-8} \text{ W/m}^2\text{-K}^4$).

According to Eqs. (1) and (2), the surface temperature of the target surface $T_S = \sqrt[4]{L_S/\sigma}$ (in Kelvin) depends on various variables. One of them is the emissivity of objects [22]. Another is the longwave radiation emitted by the background, corresponding to the skydome in most outdoor situations. The background can become more complex to define if thermal images are collected in an outdoor environment with obstructions. In this case, the longwave radiation emitted by the background can be measured from an aluminum foil placed on one of the target objects [23].

Due to the number of variables that need to be known when using an infrared camera, the accuracy of the surface temperature T_S is often less than this obtained with a contact surface sensor. However, the surface temperature T_S can be observed with a higher spatial resolution using thermal images collected by an infrared camera, as shown in Fig. 3. Therefore, thermal images enable us to evaluate how cool or hot certain elements in the built environment are compared to others. The thermal behavior of some features like trees or grass can be challenging to study with contact surface sensors, but not with thermal images. Thermal images can now be collected with a similar time resolution to contact surface sensors. Because thermal images are two-dimensional data, they require significantly more space to be stored in a computer.

3. Methodology

The objective of the review was to address one question in particular: *What are applications and research opportunities in infrared thermography at multiple scales of the built environment?* To find a response to this question, the review was conducted following the workflow described in Fig. 4. The first step in the workflow was to enter a list of keywords on the Google Scholar search engine. Among the papers resulting from the keyword-based search, one was read to understand if its content was about the built environment. The built environment refers to the outdoor environment within a city ranging in scale from the microscale to the mesoscale. Each paper, whose content corresponds to a study about the built environment, was then classified for its analysis with other contributions. The analysis was conducted after reading all the papers in the list and after using all identified keywords. From the results provided by the investigation, the objectives were to detect research opportunities and state some conclusions.

Most papers in the literature define a list of keywords they consider to be the most representative concepts discussed in their content. While reading each article, some of their keywords were considered to explore the literature further. The list of keywords used for analyzing the literature is shown in Table 1. If a paper contained one of these keywords in its list or its title, it was then considered to be potentially relevant to the review. To be fully applicable to the study, the paper also needed to address an issue of the built environment. The reason is that an article can contain one of these keywords in its list or title and discuss another topic not related to the built environment. For example,

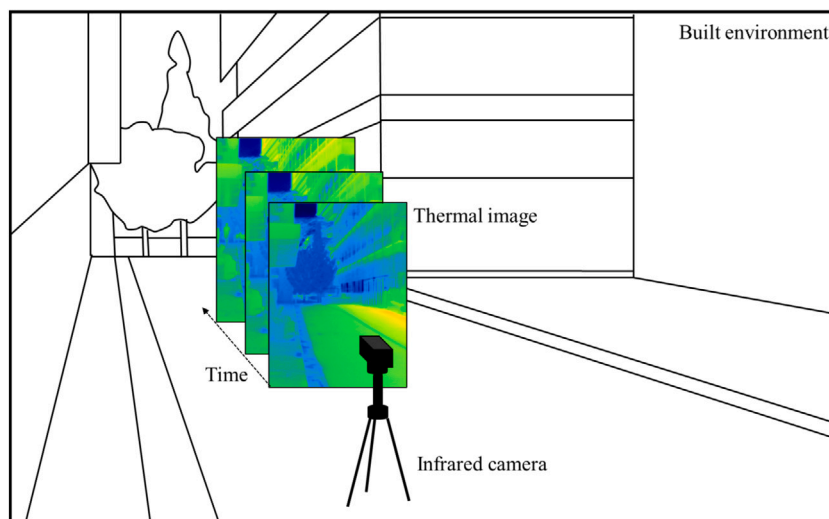


Fig. 3. Collection of thermal images using an infrared camera in the built environment.

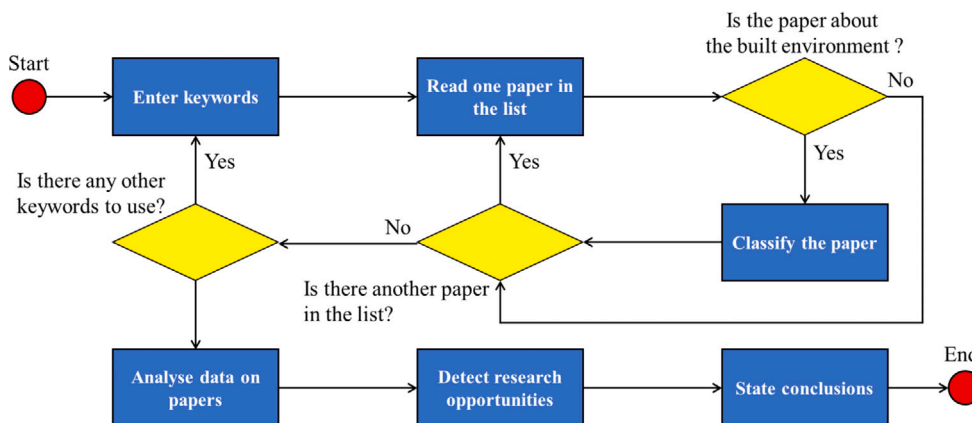


Fig. 4. Workflow used to review papers on infrared thermography for the built environment.

one paper might include the term ‘Infrared Thermography’ in its list of keywords but study one of its medical applications. In contrast, some papers might not have a word in their list of keywords and still indirectly refer to it in their content. One of the reasons is that the terminology used in infrared thermography usually varies depending on the scale it is applied. When using a satellite to collect thermal images, the term ‘Infrared Thermography’ itself is rarely used, but ‘Land surface temperature’ or ‘Remote sensing’ instead. It explains why not all reviewed papers contain the term ‘Infrared Thermography’ in their list of keywords or titles.

For each relevant contribution to the built environment, a set of information was extracted from its content. One such example is the country where the study was conducted. This piece of information enabled us to determine where most studies in infrared thermography were completed and which regions might need further exploration. Another criterion was the scale at which infrared thermography was applied in the study. In addition to the scale, it was essential to determine the system used in the study to collect thermal images and the application in which the thermal images were intended to be used. The classification of selected contributions was reported in a spreadsheet to conduct the data analysis based on all these criteria.

The scale at which a reviewed study was conducted needed more efforts to be identified than other criteria. The reason is that there are multiple ways to define the scale of a study in the built environment. One of them is described by Oke [24] and has been primarily used in urban climate studies. It includes three essential scales, which are the

mesoscale (10–200 km), the local-scale (0.1–50 km), and the microscale (>1 km). Another way to classify studies in the built environment by scales is explained by Hertwig et al. [25]. It has been used mainly by urban planners to distinguish their studies either as city-scale (10–100 km), neighborhood-scale (0.1–10 km), and building-scale (10–100 m).

Apart from comparing the number of studies for each identified class, the data analysis also consisted in understanding the evolution of infrared thermography in the built environment between 1980 and 2021. For this purpose, the chronology of selected contributions was established and analyzed to show how some limitations were overcome in the past or could be solved in the future, which explains why critique was an essential aspect of the review.

4. Results and discussion

During the literature review, it was observed that different infrared systems were used to study the built environment at one or several scales. The infrared systems are presented in Fig. 5. The system that enables the collection of thermal images at the largest scale is a satellite. Apart from the thermal images, which are usually used to measure the Land Surface Temperature (LST), a satellite can contain other sensors to collect data at the mesoscale or city-scale remotely. When thermal images are needed between the city-scale and neighborhood scales, an infrared camera is normally installed on an Aerial Vehicle (AV) such as an aircraft or a helicopter. The infrared camera can also be installed on different supports to collect thermal images at lower scales.

Table 1

Keywords used in Google Scholar search engine and the number of papers, which are relevant to the review, containing one of them in their own list of keywords or in their title.

Keyword	Number of papers
Infrared thermography	99
Heat island	46
Land surface temperature	35
Remote sensing	33
U-value	19
Unmanned aerial vehicle	12
Thermal transmittance	12
Energy efficiency	10
Buildings	10
Building envelope	9
Heat loss	9
Urban heat flux	9
Thermal bridges	8
Longwave radiation	8
Moisture	8
Thermal performance	8
3D reconstruction	8
Non-destructive testing	7
Infrared camera	6
Historic building	6
Sensible heat flux	6
Urban surface temperature	6
Urban biophysical	5
Heat mitigation	5
Thermal resistance	5
Building retrofit	5
Solar panel	4
Greenery	4
Building diagnostics	4
Cool materials	3
Laser scanning	3
Building information models	3
Net radiation	2
Building energy performance	2
Defect detection	2
Image fusion	1
Smart phone	1
Observatory	1

It is installed on a rooftop observatory for neighborhood-scale studies, on a drone for studies between the neighborhood-scale and building-scale, or with a tripod, handheld system, or smartphone for microscale studies.

Fig. 6 illustrates the number of studies that have been conducted since 1980 in the built environment using infrared thermography at different and multiple scales. In general, a growing interest in the use of infrared thermography is observed to explore the built environment, which is certainly due to major advancements of this technology and reductions in its cost. More specifically, it is seen that the portion of studies at different scales does not seem to significantly vary whether the classification of Oke [24] or Hertwig et al. [25] is used. In either case, microscale or building-scale studies appear to be the most frequent, with a portion between 50% and 55% since 1980. The number of studies conducted at the mesoscale or city scale also looks relatively substantial. However, a few contributions were found in infrared thermography to explore the built environment at the local and neighborhood scales. Even less reviewed studies considered thermal images simultaneously collected at multiple scales. The small number of local, district, and multi-scale studies can be explained from the time and cost required to collect thermal images with adequate infrared systems. Indeed, it often requires more time and cost to collect thermal images from an AV or observatory than a satellite or mounted camera.

The small portion of local-scale or neighborhood-scale studies could be explained by the fact that they are more difficult and expensive to set up than those conducted at other scales. Launching a satellite to collect

thermal images at the mesoscale or city scale might be costly, but thermal images obtained from a satellite can then be shared with the all scientific community at a relatively low price. The collection of the thermal images at the microscale or building-scale can also be achieved at a low cost whether drones, mounted cameras, handheld cameras, or smartphones are used for this purpose. In contrast, installing an infrared system to conduct a local-scale or neighborhood-scale study is always relatively expensive. Safety and confidentiality measures to consider for local-scale or neighborhood-scale studies are more important than for other scales.

Fig. 7 shows applications that can be performed in the built environment by different infrared systems and at different scales. According to review papers, thermal images collected by a satellite can be used to either observe the UHI effect, analyze urban heat fluxes, or study urban descriptors. Observations of the UHI effect were also made at the local-scale or neighborhood-scale using Aerial Vehicles (AVs), rooftop observatories, or drones. In addition, to analyze urban heat fluxes, drones were used to detect building defects, evaluate building thermal performance, analyze UHI mitigation strategies, and detect faulty Photovoltaic (PV) panels at the microscale or building scale. Similar applications were performed simultaneously using mounted cameras, handheld cameras, and smartphones.

4.1. Studies conducted at the mesoscale or city-scale

Most studies aiming at observing the built environment at the mesoscale or city-scale have used remotely sensed data collected from satellites. Between the 1950s and 1960s, satellites were essentially used for military purposes [26]. During the 1970s, several satellites were launched in orbit to collect information for the scientific community, including thermal images. The thermal images were used in some preliminary studies during the 1980s to observe the LST. For example, the accuracy with which the LST can be measured from the Landsat 3 and National Oceanic and Atmospheric Administration (NOAA) 6 was evaluated by Price [27,28]. With thermal images obtained from the NOAA 6, Price discovered that the surface temperature could be measured with an accuracy of $\pm 2-3$ °C. Other studies, such as the one by Vukovich [29], used thermal images obtained from the Heat Capacity Mapping Mission (HCMM), another satellite, to observe the difference in the LST between urban and rural areas in St. Louis (USA). In the same city, Kidder and Wu [30] made similar observations but considering the snow-covered. Later in the 2000s, two MODerate Resolution Imaging Spectroradiometer (MODIS) satellites were launched to provide a variety of remote sensed data [31]. The first satellite, MODIS Terra, was launched in 1999. It provides the same remote sensed data as the MODIS Aqua, launched in 2002.

Tables 2–4 shows reviewed studies that were conducted at the mesoscale or city-scale using infrared thermography with Landsat, NOAA, or MODIS. The majority of these studies were conducted in China and North America, as illustrated in Fig. 8 and the review of Almeida et al. [5]. A non-negligible portion of reviewed studies, approximately 12%, was conducted in Europe. These observations imply that numerous contributions in understanding the built environment at mesoscale or city-scale can still be made in several countries, particularly those located in Africa and South America.

Among all reviewed studies conducted at the mesoscale or city-scale, the majority collected thermal images from Landsat according to Fig. 9. The reason seems to be that Landsat is more suitable for observing the UHI effect and inferring urban descriptors than its concurrent. Nevertheless, MODIS Terra and Aqua look to gain interest over the years, in particular, to analyze urban heat fluxes. This fact could be due to the significant amount of remotely sensed data provided by MODIS Terra and Aqua in addition to the LST. While there was a visible competition between MODIS and Landsat in the scientific community, few reviewed studies used NOAA to understand the built environment using infrared thermography.

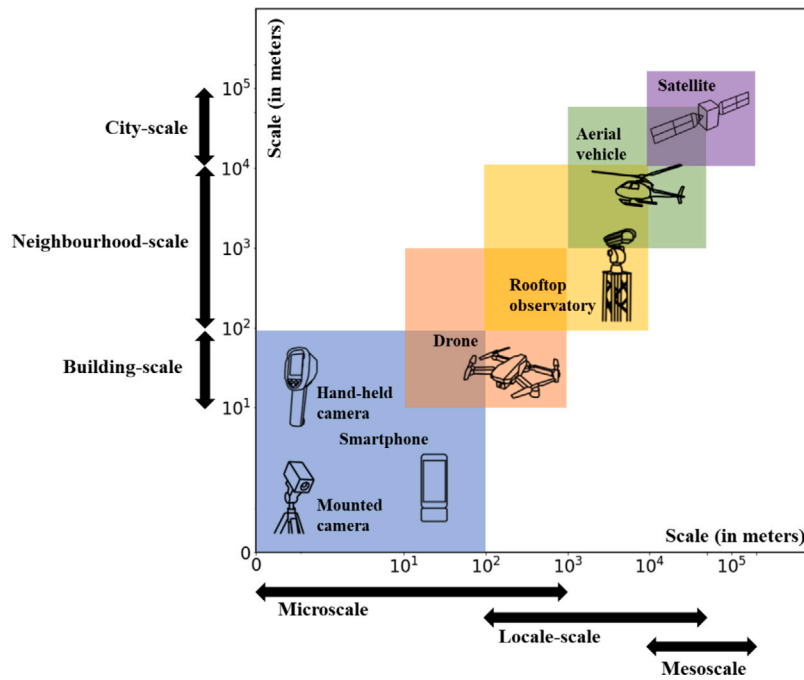


Fig. 5. Systems of infrared thermography at different scales.

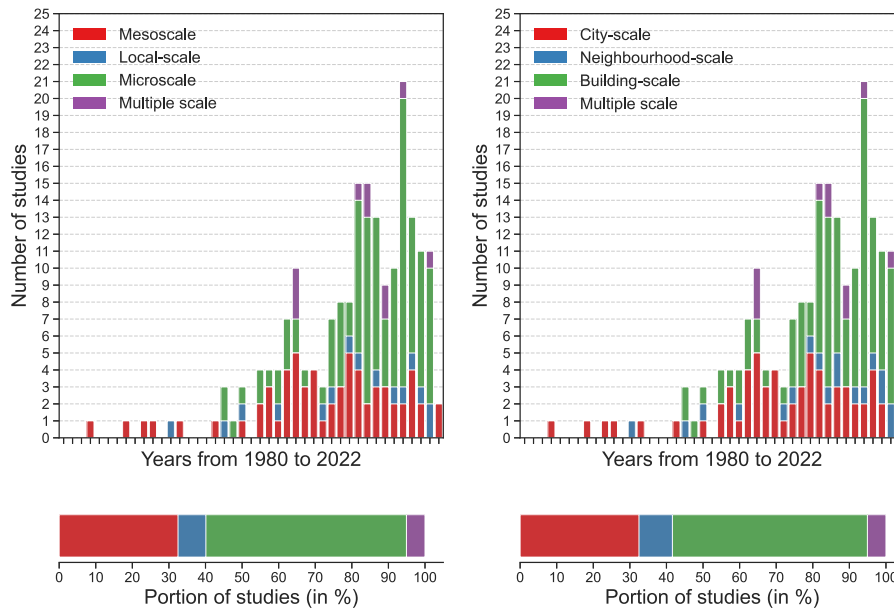


Fig. 6. Number and portion of studies between 1980 and 2022 that used infrared thermography to observe the built environment at different scales.

Fig. 10 shows the number of reviewed studies that were dedicated to observing the UHI effect, analyzing urban heat fluxes, and studying urban descriptors using thermal images collected from a satellite. According to these results, most reviewed studies aimed at observing the UHI effect using the LST measured with a satellite. A notable number of reviewed studies also used other remote sensed data in addition to the LST to analyze urban heat fluxes and study urban descriptors.

4.1.1. Observation of the UHI effect from the LST

During the 1990s and early 2000s, various studies proposed methods to observe the UHI effect from the LST measured using a satellite. Among these studies, Roth et al. [32] analyzed the UHI effect during the day and at night. The study conducted by Carnahan and Larson [33]

focused more on the possible sinks of the UHI effect. Even though thermal images can be obtained for various locations using a satellite, Roth et al. [32] and Carnahan and Larson [33] assessed the UHI effect of one city only. As an improvement, Gallo et al. [34] showed how the UHI effect could be evaluated in several cities in the United States using the NOAA satellite. Data collected using this kind of satellite can be used to develop empirical models of the UHI effect as expressed by Streutker [36]. The models can predict the UHI effect at specific times when no data is available. As illustrated by Lo and Quattrochi [37], thermal images collected from a satellite are indeed limited over time. However, the amount of information each time is relatively significant compared with what can be provided by an empirical model.

Until the early 2000s, most observations of the UHI effect at the mesoscale were reported in the United States. After the mid-2000s,

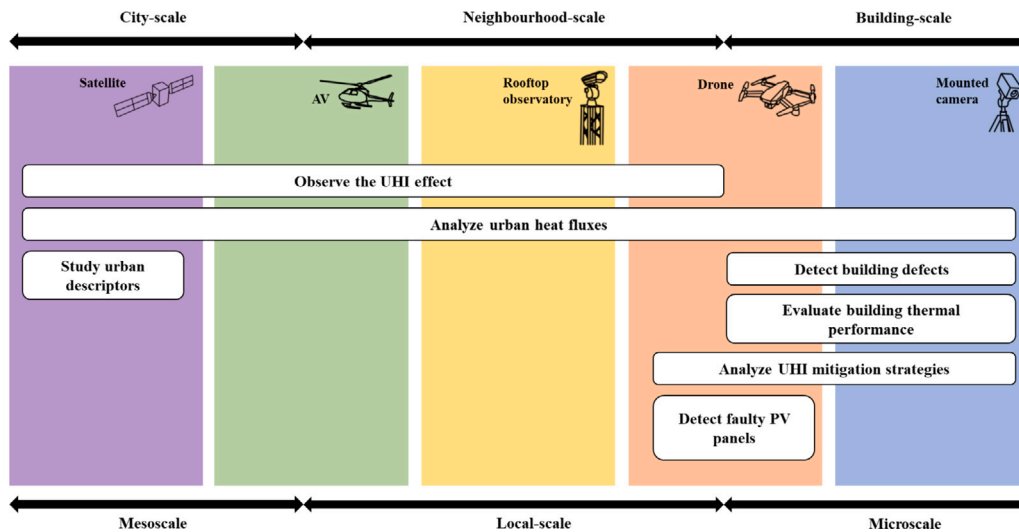


Fig. 7. Applications of infrared thermography at different scales.

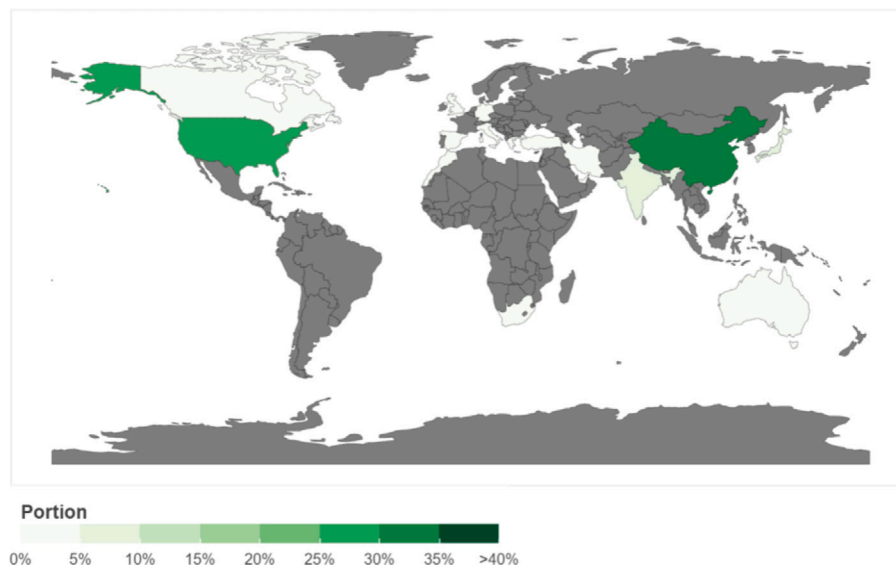


Fig. 8. Countries in which studies in infrared thermography were conducted at the mesoscale or city-scale of the built environment between 1980 and 2021.

most studies were conducted in China. For instance, Nichol [38] tried to evaluate the influence of the urban morphology of Hong Kong on the UHI effect. A more detailed study was conducted by Chen et al. [39] on the relation between the land use of Guangzhou and the UHI effect. In addition to the land use, Yang and Liu [42] retrieved biophysical characteristics using thermal images of Lanzhou to understand the formation of the UHI effect. Wang et al. [43] did not only consider thermal images to analyze the UHI effect in Beijing. They assumed the UHI effect could also be explained from the albedo, vegetation index, and broadband surface emissivity remotely sensed from MODIS. Using information measured from the Landsat Enhanced Thematic Mapper Plus (ETM+) satellite, Li and Yu [44] studied characteristics of the UHI effect in Wuhan. As a complement to the analysis based on measurements, they performed Computation Fluid Dynamics (CFD) simulations to understand how the UHI effect could be mitigated by providing better outdoor air circulation. It is relatively unusual that simulations of the UHI effect are performed in addition to a measurement-based analysis. Studies like Li et al. [46] in Shanghai and Wang et al. [63] in Shenzhen normally try to find spatial patterns and correlations using remotely sensed data from satellites to analyze the UHI effect.

Apart from the United States and China, other mesoscale studies of the UHI effect were conducted in other parts of the world during and after the 2010s. Bechtel [48] tried to identify spatial patterns of the surface temperature in Hamburg (Germany). In addition, measurements of the surface temperature were used for the classification of local climate zones following the definition established by Stewart and Oke [109]. Lazzarini et al. [53] used another kind of classification called impervious surface areas to analyze the relationship between the roughness of an urban area and the magnitude of the UHI effect in Abu Dhabi (United Arab Emirates). Despite the various classifications of an urban area that have been studied in the literature, the land use/cover seems to remain the most appropriate one to explain the UHI effect using thermal images as shown by Tomlinson et al. [52] in Birmingham (United Kingdom), Dihkan et al. [56] in Istanbul (Turkey), and Kikon et al. [59] in Noida (India). Thermal images provide information about the LST but not necessarily the ambient temperature. Because the ambient temperature is often considered to evaluate the magnitude of the UHI effect, Ho et al. [55] determined how it could be derived from thermal images obtained in Vancouver (Canada) using machine learning algorithms. A similar study was conducted by Coutts et al. [58] in Port Philip (Australia) using very high resolution airborne thermal

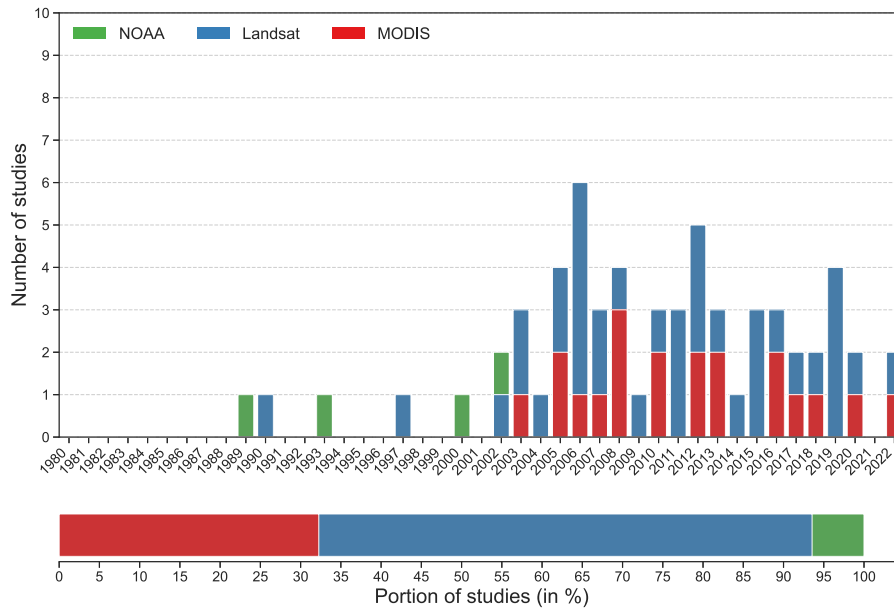


Fig. 9. Number and portion of studies between 1980 and 2022 that used either NOAA, Landsat, or MODIS to observe the built environment at the mesoscale or city-scale.

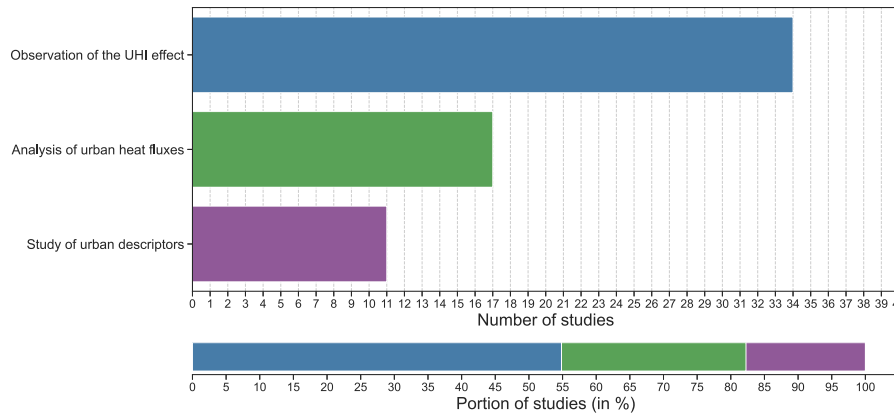


Fig. 10. Number and portion of studies between 1980 and 2022 that used a satellite to observe the UHI effect from the LST, analyze urban heat fluxes, or study urban descriptors at the mesoscale or city-scale.

images. Instead of using the difference in the surface or ambient temperature between an urban area and its rural surroundings, Shirani-Bidabadi et al. [62] used another metric called the urban heat island ratio index to calculate the magnitude of the UHI effect in Isfahan (Iran).

4.1.2. Analysis of urban heat fluxes

The analysis of urban heat fluxes tries to understand the causes of the UHI effect more than assessing its magnitude from thermal images. From the early 2000s, various studies have attempted to evaluate the heat emitted by buildings, vegetation, and anthropogenic sources from thermal images obtained by satellites.

Among these studies, some contributed to the assessment of the net-all wave radiation from remote sensing data obtained by a satellite. For example, Chrysoulakis [66] was one of the studies proposing a method to assess the net-all wave radiation, which consists of the downward shortwave radiation, the upward shortwave radiation, the downward longwave radiation, and the upward longwave radiation. A more sophisticated method was defined by Bisht et al. [68], in which the upward longwave radiation is measured from the LST and emissivity. The accuracy of the LST/emissivity method was checked by Wang et al. [70]. Tang and Li [72] describes how the net-longwave radiation can

be estimated from the upward longwave radiation assessed using the LST/emissivity method and the downward longwave radiation measured from the top of atmosphere radiance. All necessary information to compute the net-all wave radiation was measured by Bisht and Bras [74] using the MODIS Aqua satellite. Both the Aqua and Terra MODIS satellites were used by Wu et al. [76], and [80] to test multiple predictive models of the net-all wave radiation.

Apart from the net-all wave radiation, sensible and latent heat fluxes can also provide useful information to understand the causes of the UHI effect. However, these two urban heat fluxes cannot be estimated from thermal images obtained by satellite only. In addition to thermal images, data need to be collected from a network of automatic weather stations, as originally formulated by Kustas and Norman [110]. Using thermal images from satellites and data from a network of automatic weather stations, Norman et al. [64] could show one of the first pictures of latent heat fluxes at the mesoscale. Both the sensible and latent heat flux were assessed by Ma et al. [65] and French et al. [67].

Although sensible and latent heat fluxes can be directly estimated, they need to be balanced with other urban heat fluxes to ensure their validity. In the study conducted by Ma et al. [65], sensible and latent heat fluxes are balanced with the net-all wave radiation and the ground heat flux, which might not be representative of all heat

Table 2

Reviewed studies using thermal images to observe the UHI effect at the mesoscale or city-scale.

Author(s)	Year	Country	Satellite	Model(s)
Roth et al. [32]	1989	Canada	NOAA	7, 8, and 9
Carnahan and Larson [33]	1990	United States	Landsat	5
Gallo et al. [34]	1993	United States	NOAA	11
Lo et al. [35]	1997	United States	Landsat	5
Streutker [36]	2002	United States	NOAA	14
Lo and Quattrochi [37]	2003	United States	Landsat	1, 3, 4, and 5
Nichol [38]	2005	China	Landsat	7
Chen et al. [39]	2006	China	Landsat	7
Goldreich [40]	2006	South Africa	Landsat	7
			MODIS	Terra
Le-Xiang et al. [41]	2006	China	Landsat	5 and 7
Yang and Liu [42]	2006	China	Landsat	7
Wang et al. [43]	2007	China	MODIS	Aqua and Terra
Li and Yu [44]	2008	China	Landsat	7
Wan [45]	2008	China	MODIS	Aqua and Terra
Li et al. [46]	2009	China	Landsat	5 and 7
Imhoff et al. [47]	2010	United States	Landsat	7
			MODIS	Aqua
Bechtel [48]	2011	Germany	Landsat	4 and 5
Liu and Zhang [49]	2011	China	Landsat	6
Joshi and Bhatt [50]	2012	India	Landsat	5
Rhinane et al. [51]	2012	Morocco	Landsat	5
Tomlinson et al. [52]	2012	United Kingdom	MODIS	Aqua
Lazzarini et al. [53]	2013	United Arab Emirates	MODIS	Aqua and Terra
Sobrinho et al. [54]	2013	Spain	MODIS	Not available
Ho et al. [55]	2014	Canada	Landsat	5 and 7
Dihkan et al. [56]	2015	Turkey	Landsat	5 and 7
Scarano and Sobrinho [57]	2015	Italy	Landsat	8
Coutts et al. [58]	2016	Australia	MODIS	Aqua
Kikon et al. [59]	2016	India	MODIS	Terra
Li et al. [60]	2016	China	Landsat	5
Scarano and Mancini [61]	2017	Italy	Landsat	8
Shirani-Bidabadi et al. [62]	2019	Iran	Landsat	7
Wang et al. [63]	2019	China	Landsat	8

Table 3

Reviewed studies using thermal images to analyze urban heat fluxes at the mesoscale or city-scale.

Author(s)	Year	Country	Satellite	Model(s)
Norman et al. [64]	2000	United States	NOAA	Not available
Ma et al. [65]	2002	China	Landsat	5
Chrysoulakis [66]	2003	Greece	MODIS	Terra
French et al. [67]	2003	United States	Landsat	5
Bisht et al. [68]	2005	United States	MODIS	Terra
Kato and Yamaguchi [69]	2005	Japan	Landsat	5
Wang et al. [70]	2005	China	MODIS	Aqua and Terra
Kato and Yamaguchi [71]	2007	Japan	MODIS	Terra
Tang and Li [72]	2008	United States	MODIS	Aqua and Terra
Xu et al. [73]	2008	China	MODIS	Not available
Bisht and Bras [74]	2010	United States	MODIS	Aqua
Liu et al. [75]	2012	Japan	Landsat	Not available
Wu et al. [76]	2012	China	MODIS	Aqua and Terra
Weng et al. [77]	2013	United States	MODIS	Terra
Chen and Hu [78]	2017	China	MODIS	Terra
Chrysoulakis et al. [79]	2018	United Kingdom	MODIS	Terra
Qin et al. [80]	2020	China	MODIS	Aqua and Terra
Rios and Ramamurthy [81]	2022	United States	MODIS	Not available

Table 4

Reviewed studies using thermal images to study urban descriptors at the mesoscale or city-scale.

Author(s)	Year	Country	Satellite	Model(s)
Weng et al. [82]	2004	United States	Landsat	7
Lu and Weng [83]	2006	United States	Landsat	5 and 7
He et al. [84]	2007	China	Landsat	5 and 7
Zhou et al. [85]	2011	United States	Landsat	7
Xu et al. [86]	2013	China	Landsat	5
Guo et al. [87]	2015	China	Landsat	5 and 7
Scarano and Sobrinho [57]	2015	Italy	Landsat	8
Scarano and Mancini [61]	2017	Italy	Landsat	8
Sannigrahi et al. [88]	2018	India	Landsat	5 and 7
Firozjaei et al. [89]	2019	Iran	Landsat	5, 7, and 8
Ghosh et al. [90]	2019	India	Landsat	5
Hu et al. [91]	2020	China	Landsat	8
Kim et al. [92]	2022	Korea	Landsat	8

Table 5
Reviewed studies using thermal images to observe the UHI effect or analyze urban heat fluxes at the local-scale or neighborhood-scale.

Author(s)	Year	Country	Infrared camera	Model	Support
<i>Observation of the UHI effect from the LST</i>					
Eliasson [93]	1992	Sweden	AGEMA FLIR	Thermovision 870 Not available	Aircraft Aircraft
Voogt and Oke [94]	1998	Canada	AGEMA	Thermovision 880	Helicopter
Saaroni et al. [95]	2000	Israel	Not available	Not available	Helicopter
Lagouarde et al. [96]	2004	France	FLIR	SC500	Aircraft
Leuzinger et al. [97]	2010	Switzerland	InfraTec	VarioCam	Helicopter
Lagouarde et al. [98]	2013	France	FLIR	SC3000	Helicopter
Lagüela et al. [99]	2015	Spain	Xenics	Gobi-384	Drone
Honjo et al. [100]	2017	Japan	Not available	Not available	Helicopter
Antoniou et al. [101]	2019	Cyprus	FLIR	P640	Helicopter
Fabbri and Costanzo [102]	2020	Italy	FLIR	Vue Pro R	Drone
<i>Observation of the UHI effect from the UST</i>					
Lagouarde et al. [96]	2004	France	FLIR	SC500	Aircraft
Adderley et al. [103]	2015	Canada	FLIR	A40M	Observatory
Morrison et al. [104]	2020	United Kingdom	Optris	PI-160	Observatory
<i>Analysis of urban heat fluxes</i>					
Richters et al. [105]	2009	Germany	InfraTec	VarioCam	Observatory
Sham et al. [106]	2012	China	FLIR	PM 695	Observatory
Dobler et al. [107]	2021	United States	FLIR	A310	Observatory
Morrison et al. [108]	2021	United Kingdom	Optris	PI-160	Observatory

fluxes occurring in a city. For this reason, Kato and Yamaguchi [69] added the anthropogenic heat flux into the energy balance. Both the anthropogenic and ground heat fluxes were considered by Kato and Yamaguchi [71] to estimate the heat storage. The heat storage was included in the energy balance by Xu et al. [73] to obtain unsteady state predictions of urban heat fluxes.

Whether steady or unsteady state energy balance is used to assess urban heat fluxes, they can be analyzed with other sources of information. For instance, Liu et al. [75] and Weng et al. [77] studied urban heat fluxes in relation with land use maps. Another example is the study conducted by Chen and Hu [78] in which energy data were considered to improve the estimate of anthropogenic heat fluxes. It contrasts with Chrysoulakis et al. [79] who indirectly assessed anthropogenic heat fluxes from the energy balance after evaluating all other urban heat fluxes. Sensible heat fluxes were estimated by Rios and Ramamurthy [81] from many different satellite-derived and ground-based data.

4.1.3. Study of urban descriptors

In parallel to the assessment of the UHI effect and the analysis of urban heat fluxes, various studies observed urban descriptors at the mesoscale, which can either be biophysical or geometrical. Urban descriptors were inferred from remotely sensed data, including thermal images obtained by satellite, to study their impact on the LST or UHI effect.

Biophysical descriptors correspond to the different types of surfaces that can be observed over a region, including the fraction of vegetation, pavement, and soil. In the 1990s, Carlson et al. [111] and Gillies and Carlson [112] observed that biophysical descriptors could be inferred from the LST and Normalized Vegetation Difference Index (NDVI). As illustrated by these studies, the correlation between the LST and biophysical descriptors was studied initially in rural areas.

Since the 2000s, biophysical descriptors have been inferred in urban areas. Weng et al. [82] was among the first in inferring the LST and the NDVI remote sensed data to understand the correlation between the portion of vegetation in a city and its UHI effect. From the LST, Lu and Weng [83] tried to define several types of land covers from forests to highly dense urban areas.

Several studies have attempted to evaluate the impact of land cover or biophysical descriptors on the LST or UHI effect using a different method. He et al. [84] applied an interpolation between urban and rural stations to assess the UHI effect while using land cover maps estimated from satellites as in Lu and Weng [83]. Zhou et al. [85] used

a multi-linear regression model to study the impact of land cover on the LST, both obtained from a satellite. Instead of considering various biophysical descriptors, Xu et al. [86] focused on the effect caused by impervious surfaces. In contrast, Guo et al. [87] still considered several biophysical descriptors. Using an object-oriented segmentation approach, their impact was studied on clusters of the UHI effect. In addition, to assess the impact on the UHI effect, Sannigrahi et al. [88] tried to understand how some biophysical descriptors can help in mitigating this climatic hazard. A model combining a principal component analysis with an ordinary least squares regression was developed by Firozjahi et al. [89] to study the impact of biophysical descriptors on the LST. The relation between biophysical descriptors and the LST was analyzed by Ghosh et al. [90] using Geographic Information System (GIS) and statistical-based models.

Recent studies show that not only biophysical descriptors can be inferred from remotely sensed data but also geometrical ones. Among urban geometrical descriptors, sky view factors are essential in explaining the causes of the UHI effect. The lower the sky view factor is, the higher the magnitude of the UHI effect at night. The relation between the sky view factors and the LST was studied by Scarano and Sobrino [57] and Scarano and Mancini [61]. In addition to sky view factors, Hu et al. [91] analyzed how the LST is affected by many other urban geometrical descriptors. In contrast, Kim et al. [92] focused on extremely low sky view factors and their impact on the LST.

4.2. Studies conducted at the local-scale or neighborhood-scale

Compared to the mesoscale or city-scale, more infrared systems can be used to observe the built environment at the local or neighborhood scales. In Fig. 11, it is shown that the built environment was observed mainly using an infrared camera installed on a helicopter or observatory. The use of aircraft can utilize expensive platforms to collect thermal images at the local or neighborhood scales. Drones are a modern technology, which appears to be used in a few studies at the local or neighborhood-scale for the moment, but might gain more interest in the future due to its low cost in comparison to other systems.

As observed at the mesoscale or city-scale, and as illustrated in Fig. 12, most studies at the local-scale or neighborhood scale aim at observing the UHI effect and analyze urban heat fluxes using thermal images. The only difference is that the UHI effect can either be observed from the LST or UST at a local or neighborhood scale. This observation is explained by the fact that infrared systems like helicopters and

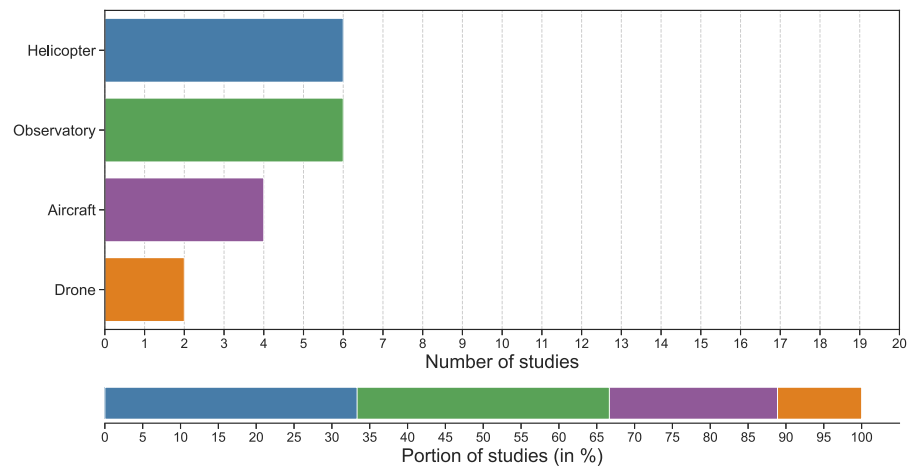


Fig. 11. Number and portion of studies between 1980 and 2022 that used either an aircraft, helicopter, observatory, or drone to observe the built environment at the local-scale or neighborhood scale.

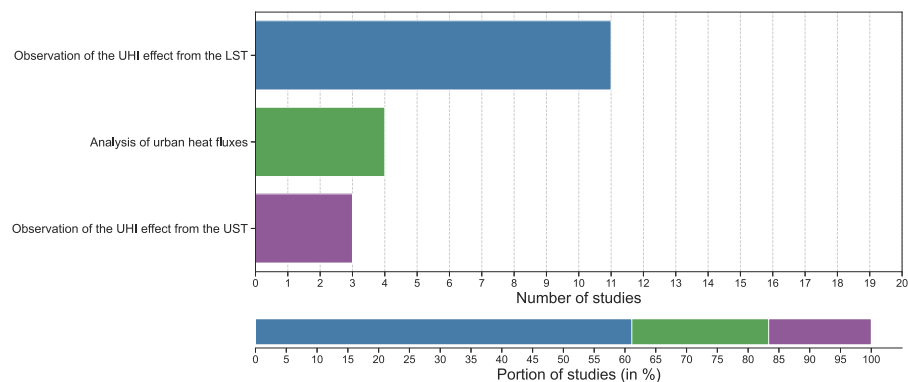


Fig. 12. Number and portion of studies between 1980 and 2022 that used thermal images to observe the UHI effect from the LST or UST and analyze urban heat fluxes at the local-scale or neighborhood scale.

observatories enable the collection of thermal images from different perspectives, including an oblique or vertical view of an urban area. It implies that thermal images collected at the local or neighborhood scale can potentially provide more information about the magnitude or causes of the UHI effect than at other scales. Because of this, it is surprising that a few efforts have been made so far to investigate the UHI effect using infrared thermography at the local scale or neighborhood scale (see Table 5).

4.2.1. Observations of the UHI effect from the LST

In Section 4.1.1, it was discussed that many studies had collected thermal images to observe the LST or UHI effect of a city. Thermal images collected from a satellite have a limited resolution, which can distort observations of the LST at the local scale.

For this reason, various studies have collected thermal images either from an aircraft or helicopter. Eliasson [93] was among the first studies in observing the LST measured from two infrared cameras that were placed on an airplane. Instead of an aircraft, Voogt and Oke [94] preferred to use a helicopter to collect thermal images at the local scale.

These two studies were considered as references to many others that have been conducted since the 2000s. Saaroni et al. [95], for example, show how characteristics of the UHI effect at the local scale can be obtained from an infrared camera installed on a helicopter and a network of automatic weather stations. The view of thermal images collected from an aircraft or a helicopter is not necessarily planned but can also be oblique as shown in Lagouarde et al. [96]. From a plan view, Leuzinger et al. [97] observed the surface temperature of different species of trees in an urban area.

Aircraft and helicopters are constantly in motion, which does not facilitate the collection of thermal images over space and time. Concerning this problem, Lagouarde et al. [98] explains how time-series can be extracted from thermal images obtained from a helicopter. Honjo et al. [100] tried to reconstitute an LST map from a mosaic of thermal images taken at different positions from a helicopter. A similar map was used by Antoniou et al. [101] to validate the LST assessed from computational fluid dynamics.

It might be relatively expensive to use an aircraft or helicopter to collect thermal images at the local or neighborhood scales. For this reason, other studies explored the possibility of using drones for this purpose. To reconstitute thermal image at the local-scale or neighborhood-scale, drones need to travel at several points over the region of interest as explained by Lagüela et al. [99] and Fabbri and Costanzo [102].

4.2.2. Observations of the UHI effect from the UST

As shown by Lagouarde et al. [96], the Urban Surface Temperature (UST) can partially be obtained from thermal images obtained by an aircraft or helicopter. By UST, it is here referred to the surface temperature of façades, roofs, and streets in an urban area as formulated by Krayenhoff and Voogt [113].

Instead of using an aircraft or helicopter, studies measured the UST from an infrared camera installed at the rooftop of a building. This type of installation is often referred to as an observatory. An observatory with pan/tilt unit was installed by Adderley et al. [103], for instance, to collect hemispheric thermal images over 360 degrees. Using a similar infrared system, but without a pan/tilt unit, Morrison et al. [104] observed the UHI effect from the UST of an entire neighborhood.

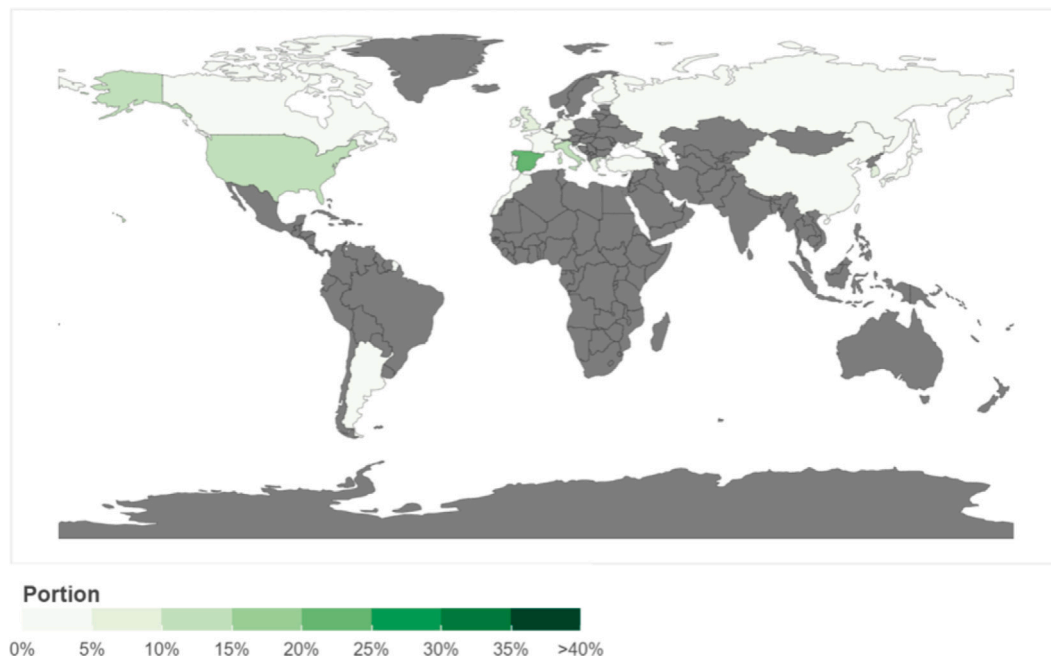


Fig. 13. Countries in which studies in infrared thermography were conducted at the microscale or building-scale of the built environment between 1980 and 2021.

4.2.3. Analysis of urban heat fluxes

Thermal images collected from an observatory can also assess urban heat fluxes at the local or neighborhood scales. Apart from the heat emitted by roofs and roads, which is better assessed using thermal images collected from an aircraft or helicopter, observatories enable to improve estimates of heat fluxes coming from building façades or any other vertical element in an urban area. Studies conducted by Richters et al. [105] and Morrison et al. [108] prove that estimates of the longwave radiation emitted by building façades can be improved using an observatory. Another urban heat flux, the sensible heat emitted by building façades, was observed by Sham et al. [106] using an observatory and a network of automatic weather stations. According to Dobler et al. [107], thermal images collected by an observatory also allow locating the heat emitted by HVAC systems.

4.3. Studies conducted at the microscale or building-scale

As mentioned at the beginning of Section 4, the majority of observations in the built environment using infrared thermography were made at the microscale or building-scale. Fig. 13 shows that a significant portion of these observations was made in Europe, in particular Spain and Italy. In Asia and North America, as well, several studies in the built environment were performed at the microscale or building-scale. As observed for studies conducted at the mesoscale or city-scale, South America and Africa are the regions where more efforts should be made in the future.

Most studies at the microscale or building-scale were performed using an infrared camera mounted on a tripod, as illustrated in Fig. 14. A non-negligible number of studies were conducted using handheld cameras or drones. Smartphones, however, do not seem to have been considered by many studies to collect thermal images of the built environment. A possible explanation would be that infrared cameras and software integrated into smartphones are not yet as performant as those included in mounted, handheld, or drone systems.

Fig. 15 demonstrates that more than 85% of reviewed studies at the microscale or building-scale were conducted to detect defects of buildings or evaluate their thermal performance. The other 20% of studies were dedicated to analyzing mitigation strategies of the UHI effect, detecting defects on PV panels, observing techniques to renovate

buildings, and analyzing urban heat fluxes. The latter application is the only one that can also be found in studies conducted at higher scales. It implies that studies performed at the microscale or building-scale are more concerned by aspects that can affect the building energy efficiency. At the same time, those conducted at higher scales give more attention to phenomena impacting the outdoor environment.

The detection of defects appears to have been performed on residential buildings mainly and on historical ones a little. Fig. 16 also show that none of the reviewed studies considered defects that might appear on the envelope of office or commercial buildings. This gap can certainly be justified by the fact that most studies at the microscale or building-scale were conducted in Europe, where a considerable portion of the energy is consumed in residential buildings D'Agostino et al. [114]. However, it was reported by Berardi [115] that the energy demand in non-residential buildings increases in Europe, as well as in other regions of the globe. The fact that few observations were made on the energy performance of non-residential buildings can then become a considerable limitation in the building sector (see Tables 6–8).

4.3.1. Detection of defects on residential or historical buildings

In infrared thermography, defects of a building primarily refer to all imperfections on its envelope that can compromise its indoor thermal comfort and energy efficiency. Grinzato et al. [116] were among the first in listing all building defects that can be detected from an infrared camera at the micro-scale or building-scale. It includes plaster detachment on walls, insulation deficiencies, thermal bridges, and moisture. These defects were detected by Grinzato et al. [116] as anomalies in thermal images provided by the infrared camera.

Techniques to detect defects were originally studied on historical or old buildings' envelopes or structural elements. For example, Haralambopoulos and Paparsenos [117] tried to detect insulation deficiencies on the envelope of an old building located in Salonika (Greece). A similar method was used by Grinzato et al. [119,130], Al-Kassir et al. [122], Tavukçuoğlu et al. [124], and Kordatos et al. [131] to observe damages caused moisture on the façade of ancient buildings. Instead of considering the entire envelope of a building, Li et al. [118] studied defects caused by air gaps or moisture on ceramic tiles. Studies like Rosina et al. [120] and Edis et al. [138,141] also focused on damages caused by moisture on structural elements. Lerma et al. [139] determined

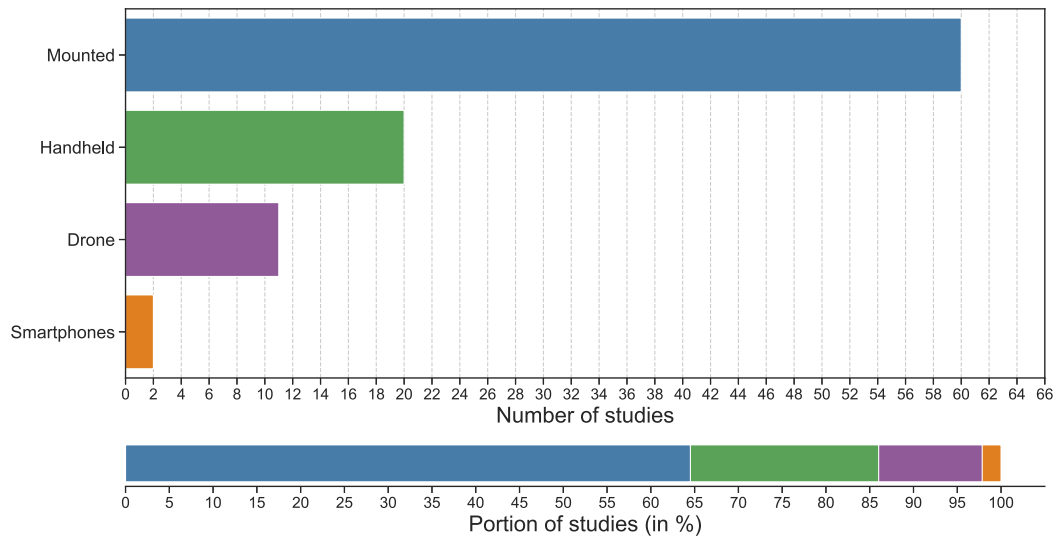


Fig. 14. Number and portion of studies between 1980 and 2022 that used mounted cameras, handheld cameras, smartphones, or drones to observe the built environment at the microscale or building-scale.

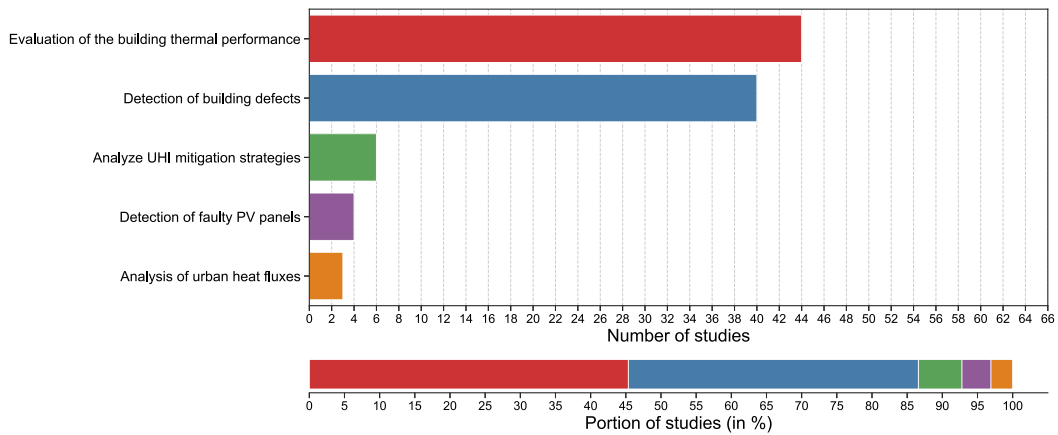


Fig. 15. Number and portion of studies between 1980 and 2022 that used thermal images to detect building defects, evaluate building thermal performance, analyze UHI mitigation strategies, detect faulty PV panels, observe renovated buildings, and analyze urban heat fluxes at the microscale or building-scale.

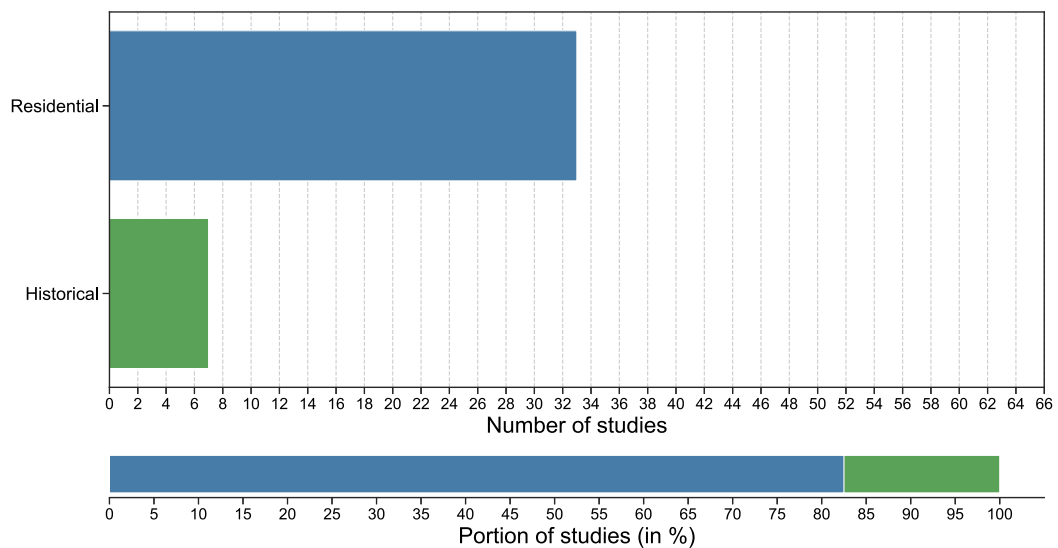


Fig. 16. Number and portion of studies between 1980 and 2022 that used thermal images to detect defects on residential or historical buildings at the microscale or building-scale.

Table 6
Reviewed studies using thermal images to detect defects on residential or historical buildings at the microscale or building-scale.

Author(s)	Year	Country	Infrared camera	Model	Support
Grinzato et al. [116]	1998	Finland	Not available	Not available	Mounted
Haralambopoulos and Paparsenos [117]	1998	Greece	Not available	Not available	Mounted
Li et al. [118]	2000	China	Not available	Not available	Mounted
Grinzato et al. [119]	2002	Italy	Not available	Not available	Mounted
Rosina et al. [120]	2003	United States	Not available	Not available	Mounted
Ocaña et al. [121]	2004	Spain	FLIR	SC2000	Mounted
Al-Kassir et al. [122]	2005	Spain	Not available	Not available	Mounted
Meola et al. [123]	2005	Italy	FLIR	SC3000	Mounted
Tavukçuoğlu et al. [124]	2005	Turkey	AGEMA	550	Mounted
Martinez-De Dios and Ollero [125]	2006	Spain	FLIR	P20	Drone
Meola [126]	2007	Italy	FLIR	SC3000	Mounted
Ribarić et al. [127]	2009	Croatia	FLIR	PM695	Mounted
Vavilov [128]	2010	Russia	Not available	Not available	Mounted
Zalewski et al. [129]	2010	France	AGEMA	PM 570	Mounted
Grinzato et al. [130]	2011	Italy	Not available	Not available	Mounted
Kordatos et al. [131]	2013	Greece	FLIR	T360	Mounted
Cerdeira et al. [132]	2011	Spain	FLIR	Not available	Mounted
Lerma et al. [133]	2011	Belgium	FLIR	B4	Handheld
Avdelidis and Moropoulou [134]	2004	Greece	AVIO	Not available	Mounted
Hopper et al. [135]	2012	United Kingdom	FLIR	B365	Mounted
Paoletti et al. [136]	2013	Italy	FLIR	S65	Mounted
Bianchi et al. [137]	2014	Italy	FLIR	Not available	Mounted
Edis et al. [138]	2014	Portugal	FLIR	B2	Handheld
Lerma et al. [139]	2014	Spain	FLIR	B335	Mounted
Taylor et al. [140]	2014	United Kingdom	FLIR	Not available	Mounted
Edis et al. [141]	2015	Turkey	FLUKE	TiR27	Mounted
Fox et al. [142]	2015	United Kingdom	FLIR	T620bx	Mounted
Lai et al. [143]	2015	China	FLIR	SC3000	Mounted
Barreira et al. [144]	2016	Portugal	Not available	Not available	Mounted
Fox et al. [145]	2016	United Kingdom	FLIR	T620bx	Mounted
Barreira et al. [146]	2017	Portugal	Not available	Not available	Mounted
Marino et al. [147]	2017	Argentina	FLUKE	TiR32	Handheld
O'Grady et al. [148]	2017	Ireland	FLIR	T335	Mounted
Baldinelli et al. [149]	2018	Italy	FLIR	B360	Mounted
Bauer et al. [150]	2018	Germany	FLIR	T420	Mounted
Mauriello [151]	2018	United States	FLIR	FLIR One	Smartphone
O'Grady et al. [152]	2018	Ireland	FLIR	T335	Mounted
Tejedor et al. [153]	2020	Spain	NEC	TH9100MR	Mounted
Rakha et al. [154]	2021	United States	FLIR	Zenmuse X2	Drone

whether damages caused by moisture on structural elements can be identically detected in a laboratory or on-site. Other types of defects on structural elements were analyzed by Meola et al. [123], Meola [126], and Cerdeira et al. [132], including cork diskettes and air-filled plastic bags.

Since the early 2000s, numerous studies have aimed at detecting locations on the envelope of a building where heat can escape from the indoor to the outdoor, that is, heat losses. One of the main source of heat losses are windows as demonstrated by Ocaña et al. [121], Vavilov [128], Barreira et al. [146], and Marino et al. [147]. Some windows can be difficult to observe from a mounted or handheld camera. For this reason, Martinez-De Dios and Ollero [125] used a drone to detect heat losses from the windows of a tall building. In addition to windows, Ribarić et al. [127] captured heat losses from heat exhausts using both thermal and Red–Green–Blue (RGB) images.

Some building defects are not necessarily detected at a specific instant. They are sometimes the result of degradation over time, which requires a multi-temporal analysis of thermal images for their detection. A multi-temporal analysis was performed by Lerma et al. [133] to better locate damages caused by moisture on the façade of a historical building. The same kind of analysis was performed by Fox et al. [142] and Bauer et al. [150] to detect cracks that might appear on residential buildings over time. A large and long experimental campaign was conducted by Barreira et al. [144] to assess all moisture-based defects that can appear on structural elements of the built environment. Fox et al. [145] reported various defects that can gradually appear outside or inside a building and detect by infrared thermography. Apart from imperfections that gradually appear over time, some degradation caused by a sudden event like debonds on an external wall can be seen from a multi-temporal analysis as proven by Lai et al. [143].

Although moisture appears to be the main cause of defects on the envelope of a building, it can also be provoked by other phenomena. For example, Paoletti et al. [136] studied damages resulting from an earthquake.

Instead of detecting defects appearing on the envelope of buildings, certain studies focused on damages caused by renovation or retrofitting. Among these studies, Avdelidis and Moropoulou [134] described several of these renovation methods applied on historical buildings, which includes surface cleaning, consolidation of stones, restoration of mortars, and examination of plaster mosaics. Another study is the one conducted by Hopper et al. [135], in which thermal bridges that might emerge after retrofitting are detected using infrared thermography.

Thermal bridges are among the most complex defects to detect from a thermal image. The reason is that it requires an assessment of the heat conduction through the envelope of a building as reported by Bianchi et al. [137] and O'Grady et al. [148]. Zalewski et al. [129], Taylor et al. [140], and O'Grady et al. [152] linked infrared thermography with computer simulation to analyze thermal bridges on the envelope of a building or specific structural elements. Thermal bridges can be quantified using an incidence factor as expressed by Baldinelli et al. [149]. Instead of using a single metric like the incidence factor, Tejedor et al. [153] detected thermal bridges from a 2D map of U-values assessed from an infrared camera. A 3D thermal model of a building was created by Rakha et al. [154] from a drone to detect thermal bridges on the envelope.

4.3.2. Evaluation of building thermal performance

The thermal performance of a building corresponds to its capability to maintain indoor conditions at a satisfactory level of thermal comfort

Table 7
Reviewed studies using thermal images to evaluate building thermal performance at the microscale or building-scale.

Author(s)	Year	Country	Infrared camera	Model	Support
Albatici and Tonelli [155]	2010	Italy	Not available	Not available	Mounted
Fokaides and Kalogirou [20]	2011	Cyprus	FLIR	T360	Handheld
Lagüela et al. [156]	2011	Spain	NEC	TH9260	Mounted
Lagüela et al. [157]	2013	Spain	NEC	TH9260	Mounted
Dall'O et al. [158]	2013	Italy	FLIR	T640bx	Mounted
González-Aguilera et al. [159]	2013	Spain	NEC	TH9260	Mounted
Ham and Golparvar-Fard [160]	2013	United States	FLIR	E60	Handheld
Lagüela et al. [161]	2013	Spain	NEC	TH9260	Mounted
Lehmann et al. [162]	2013	Switzerland	NEC	TH3102	Mounted
Wang et al. [163]	2013	United States	Not available	Not available	Mounted
Baldinelli and Bianchi [164]	2014	Italy	FLIR	Not available	Mounted
Lagüela et al. [165]	2014	Spain	Xenics	Gobi384	Drone
Lagüela et al. [166]	2014	Spain	NEC	TH9260	Mounted
Wakili et al. [167]	2014	Switzerland	NEC	TH770	Mounted
Albatici et al. [168]	2015	FLIR	Not available	Not available	Mounted
Ham and Golparvar-Fard [169]	2015	United States	FLIR	E60	Mounted
Nardi et al. [170]	2015	Italy	FLIR	S65	Mounted
Gaspar et al. [171]	2016	Spain	FLIR	E60bx	Handheld
Kim et al. [172]	2016	South Korea	FLIR	T620	Mounted
Choi and Ko [173]	2017	South Korea	FLIR	T620	Mounted
Marino et al. [147]	2017	Argentina	FLUKE	TiR32	Handheld
Maroy et al. [174]	2017	Belgium	Not available	Not available	Mounted
Tejedor et al. [175]	2017	Spain	FLIR	E60bx	Mounted
Baffa [176]	2018	Canada	Testo	T870	Handheld
Bienvenido-Huertas et al. [177]	2018	Spain	FLIR	E60bx	Handheld
Gaspar et al. [178]	2018	Spain	FLIR	E60bx	Handheld
Marshall et al. [179]	2018	United Kingdom	FLIR	B425	Mounted
Mauriello [151]	2018	United States	FLIR	FLIR One	Smartphone
Tejedor et al. [180]	2018	Spain	FLIR	E60bx	Handheld
Yang et al. [181]	2018	Taiwan	FLIR	FLIR One	Smartphone
Bienvenido-Huertas et al. [182]	2019	Spain	FLIR	E60bx	Handheld
Choi and Ko [183]	2019	South Korea	FLIR	T620	Mounted
Gaši et al. [184]	2019	Croatia	FLIR	Not available	Mounted
Lu and Memari [185]	2019	United States	Testo	875-1i	Mounted
Sen and Al-Habaibeh [186]	2019	United Kingdom	IRISYS	1002	Mounted
Tejedor et al. [187]	2019	Spain	FLIR	E60bx	Handheld
Sadhukhan et al. [188]	2020	United States	FLIR	Not available	Drone
Tejedor et al. [189]	2020	Spain	FLIR	E60bx	Handheld
Tejedor et al. [153]	2020	Spain	NEC	TH9100MR	Mounted
Bayomi et al. [190]	2021	United States	FLIR	Zemuse X2	Drone
Mahmoodzadeh et al. [191]	2021	Canada	FLIR	A65	Mounted
Papadakis et al. [192]	2021	Greece	FLIR	B40	Handheld
Park et al. [193]	2021	South Korea	Not available	Not available	Mounted
Tejedor et al. [194]	2021	Spain	FLIR	Not available	Mounted
Rakha et al. [154]	2021	United States	FLIR	Zemuse X2	Drone

with the presence or absence of defects on its envelope. The most common metric to quantify the thermal performance of a building is its thermal transmissivity or U-value. Since the 2010s, various studies have used infrared thermography at the microscale or building-scale to assess the U-value of buildings. Albatici and Tonelli [155] and Albatici et al. [168] were among the first in estimating the U-value of residential buildings from thermal images. More complex methods were then developed as in Bienvenido-Huertas et al. [177], Gaspar et al. [178], Choi and Ko [183], Lu and Memari [185], Tejedor et al. [189], and Mahmoodzadeh et al. [191]. Using infrared thermography, the U-value can also be studied in two dimensions as demonstrated by Tejedor et al. [194].

Any method to calculate the U-value from thermal images is usually validated estimates with measurements of the surface temperature obtained by contact sensors. It was shown that the accuracy of the U-value could be improved using aluminum foil as in Fokaides and Kalogirou [20], Dall'O et al. [158], Tejedor et al. [180], and Papadakis et al. [192]. The aluminum foil is placed on the building envelope to measure the background temperature, which is a crucial variable to measure the surface temperature from an infrared camera accurately. Besides the background temperature, the U-value assessed from thermal images is also sensitive to outdoor conditions as proven by Lehmann et al. [162], Wakili et al. [167], and Kim et al. [172]. Nardi et al. [170], Gaspar et al. [171], Choi and Ko [173], Tejedor et al. [175], Baffa [176], Bienvenido-Huertas et al. [182], and Gaši et al.

[184] compared different methods to estimate the U-value using a mounted or handheld camera. In contrast, Bayomi et al. [190] used a drone to assess the U-value of the building enveloped from thermal images.

Indeed, the U-value is typically obtained from thermal images of an opaque surface. It is relatively difficult to assess the U-value of transparent surfaces like the glass on windows. Despite this difficulty, Baldinelli and Bianchi [164], Maroy et al. [174], and Park et al. [193] attempted to infer the U-value of various types of glazing using an infrared camera and compared estimates with measurements collected by contact sensors.

Instead of using the U-value, other studies analyzed the thermal performance of buildings from 3D thermal models. As illustrated by Lagüela et al. [156], a 3D thermal model aims at capturing the thermal behavior of a building from all possible angles. In the literature, several techniques were explored to generate 3D thermal models. One of them consists of fusing and matching thermal images collected from different angles as defined by Lagüela et al. [157], González-Aguilera et al. [159], and Yang et al. [181]. Instead of fusing and matching a sequence of thermal images, Ham and Golparvar-Fard [160] and Wang et al. [163] generated a cloud of geolocalized points, whose surface temperature was captured by an infrared camera at different positions. Whether the 3D thermal model is obtained by fusion/matching or a cloud of points, Lagüela et al. [161] shows that it can be integrated into Building Information Modelling (BIM) to analyze the thermal

Table 8
Reviewed studies using thermal images for other applications at the microscale or building-scale.

Author(s)	Year	Country	Infrared camera	Model	Support
<i>Analysis of strategies to mitigate the UHI effect</i>					
Mastrapostoli et al. [195]	2016	Greece	AGEMA	Not available	Mounted
Monteiro et al. [196]	2017	Portugal	NEC	TH7800	Handheld
Chui et al. [197]	2018	United States	FLIR	T650sc	Handheld
Kolokotsa et al. [198]	2018	Greece	FLIR	B2	Handheld
Garcia-Nevaldo et al. [199]	2020	Spain	FLIR	T460	Mounted
Cho et al. [200]	2021	South Korea	FLIR	Vue Pro R	Drone
<i>Detection of faulty PV panels</i>					
Lee et al. [201]	2018	South Korea	Not available	Not available	Drone
Ismail et al. [202]	2019	United Arab Emirates	FLIR	Zenmuse XT	Drone
Et-taleby et al. [203]	2020	Morocco	Not available	Not available	Drone
Henry et al. [204]	2020	South Korea	FLIR	Vue Pro R	Drone
<i>Analysis of urban heat fluxes</i>					
Hoyano et al. [205]	1999	Japan	Not available	Not available	Mounted
Feng et al. [206]	2019	China	FLIR	Vue Pro 640R	Drone
Arjunan et al. [207]	2021	Singapore	FLIR	A300	Mounted

performance of a building. After integrating the 3D thermal model into BIM, Lagüela et al. [166] assessed the U-value for each surface of the building. Ham and Golparvar-Fard [169] created an entire 3D map of U-values and integrated it into BIM. Instead of using BIM, Marshall et al. [179] used another building visualization model to fix the 3D map of U-values.

Recently, some efforts have been made to evaluate the thermal performance of a building using thermal images and artificial intelligence. Sen and Al-Habaibeh [186] could categorized different types of walls using an artificial neural network and the U-value calculated from thermal images. The U-value of different walls was also studied by Tejedor et al. [187] through time series analysis. An instance segmentation technique was used by Sadhukhan et al. [188] to estimate the U-value of various elements on a building, including doors, walls, and windows.

4.3.3. Analysis of strategies to mitigate the UHI effect

While the UHI effect is generally observed at the mesoscale or city-scale, strategies to mitigate its aggravation are usually studied at the microscale or building scale. The main reason is that it would be time-consuming and expensive to set up an experiment on UHI mitigation strategies at the mesoscale or city scale.

Despite the emergency in finding solutions to mitigate the UHI effect, it was observed that a few reviewed studies were dedicated to their analysis using infrared thermography. Among the studies that used infrared thermography to analyze mitigation strategies of the UHI effect, Mastrapostoli et al. [195] and Cho et al. [200] could capture the effect and deterioration of cool roofs over time. An alternative to cool roofs is rooftop gardens, whose influence was studied by Monteiro et al. [196] using a sequence of thermal images collected at different positions. The UHI effect is not necessarily mitigated using strategies on the roof of buildings. Chui et al. [197] and Kolokotsa et al. [198], for instance, observed how certain materials enable to reduce the surface temperature of street pavements using infrared thermography. The surface temperature of the street pavement can also be reduced using shading devices as shown by Garcia-Nevaldo et al. [199].

4.3.4. Detection of faulty PV panels

Recently, various studies have tried to detect faulty PV panels using infrared cameras installed on drones. As for defects on the envelope buildings, Lee et al. [201], Ismail et al. [202], and Henry et al. [204] detect faulty PV panels from anomalies on thermal images. A more sophisticated method relying on machine learning was developed by Et-taleby et al. [203] to automatically detect faulty PV panels.

4.3.5. Analysis of urban heat fluxes

Among all applications of infrared thermography in the built environment, the analysis of urban heat fluxes is the only one that could be found at multiple scales. However, more studies can be found at higher scales than at the microscale or building scale. Among the few studies conducted at the microscale or building-scale, Hoyano et al. [205] analyzed the sensible heat emitted by a building over a typical day. Sensible heat fluxes were also studied by Feng et al. [206] from thermal images collected by a drone. Arjunan et al. [207] observed the operation of HVAC systems using infrared thermography; and, thus, indirectly assessed the anthropogenic heat that might be emitted from the use of air conditioning.

4.4. Multi-scale studies

Although many contributions have been made in infrared thermography at different scales of the built environment, a small number considered multiple scales in the same study. One of them is the study conducted by Gluch et al. [208] in the early 2000s. The objective was to compare thermal images obtained at the mesoscale with others collected at the microscale. A similar comparison was made by Golden and Kaloush [209] and Hartz et al. [210], but at the city-scale using a satellite and at the building-scale using a handheld infrared camera.

It might be abrupt to directly compare thermal images obtained at a very large scale with these collected at a smaller scale. For this reason, Yamazaki et al. [211] decided to study the UHI effect between the local-scale and microscale. Other studies like Kuo et al. [212] and Parlow et al. [213] preferred to consider thermal images obtained at the mesoscale and local scale. Bonafoni et al. [214] and Bonafoni and Tosi [215] developed a downscaling method to collect thermal images of the built environment from the city-scale to the building scale.

5. Research opportunities

During the review, several research opportunities were identified at different scales of the built environment. The next phase of research should explore the convergence of infrared radiation data with Internet-of-Things (IoT), geospatial data, and other data sources found in the built environment. This foundation enables the use of infrared thermography for applications at the urban scale, such as energy modeling and the UHI effect. Although the UHI effect was observed using infrared thermography in numerous studies, in particular at the mesoscale, some improvements can still be made in the future.

5.1. Temporal data integration with Internet-of-Things (IoT) and other imaging systems

Infrared thermography images taken over a period of time results in the collection of surface temperature data with a temporal dimension. These data enable the extraction of behavior related to the dynamics of building envelopes, mechanical systems, and human behavior in buildings. Collection of the temporal dynamics from these systems empowers the convergence of data from other types of energy, indoor and outdoor environmental quality, and wearable measurements. Additionally, data from infrared data collection could be linked with other remote sensing systems such as visible light, broadband, and hyperspectral imaging to achieve high-level insights about numerous buildings simultaneously. An example of such a deployment is the Urban Observatory that was deployed in New York City, which was able to capture the energy consumption, lighting use, grid stability, and environmental conditions of hundreds of buildings on the Manhattan skyline at once [107]. This data fusion also enabled the evaluation of urban vegetative health, the ecological impacts of light pollution, and the technology adoptions habits of building occupants.

5.2. Geospatial data integration and digital twins

As large-scale data sourced from infrared thermography is essentially a form of geospatial data, the literature review exposed a notable gap of the lack of recognition of such data in the geospatial realm, its integration in GIS, and coupling it with other kinds of geoinformation, potentially uncovering new applications in the built environment. With digital twins increasingly supporting dynamic data and allowing accommodating diverse sources [216,217], a viable research direction would be to investigate the direct integration of latent thermal data in them, potentially facilitating new use cases, e.g., understanding urban vibrancy and thermal comfort [218,219]. For example, the standard CityJSON [220] enables extending urban digital twins with new types of information. A direction for future work would be researching an automated way to supplement the standard with static or dynamic information from thermal cameras and associate them with urban features that are already available in these datasets.

Another notable development at the urban scale and in the geospatial domain is the proliferation of street view imagery [221–223]. Since thermal cameras may be mobilized, a question that arises is whether we can develop a new research line that focuses on developing street-level thermal imagery, supplementing optical imagery, which has been the main focus of research so far [224].

As advances in computer vision provide means to process a large number of images and as these techniques are gaining momentum in urban studies [225–228], it might be worthwhile to use them to develop new mechanisms to process thermal imagery and reveal new applications.

5.3. Detailed and comparative analysis of urban heat fluxes at multiple scales

As discussed in Section 4, the analysis of urban heat fluxes is an application of infrared thermography that can certainly be used to explore the built environment at multiple scales. Nonetheless, it was observed that the level of detail with which urban heat fluxes were analyzed varies concerning the scale they were studied. At the mesoscale or city-scale, highly detailed observations of urban heat fluxes were made using thermal images and other remote data collected from satellites. At lower scales, only a few urban heat fluxes were considered by reviewed studies at the same time. Most of these studies essentially inferred the sensible and anthropogenic heat emitted by buildings from thermal images.

While urban heat fluxes were considered at different scales separately, none of the reviewed studies compared their estimates at

multiple scales simultaneously. To perform this kind of comparison would also require the deployment of automatic weather stations at various scales. It would also be recommended to use and synchronize several infrared systems. Such a network of infrared systems and automatic weather stations have not been deployed over a city.

Therefore, there are two main research opportunities related to the analysis of urban heat fluxes at multiple scales. One possibility would be to perform a more detailed analysis of urban heat fluxes at lower scales than the mesoscale or city-scale by considering the latent heat emitted by vegetation or the anthropogenic heat released by traffic, for instance. Another opportunity would be to compare urban heat fluxes estimated from thermal images at multiple scales and evaluate their divergence.

5.4. Urban-scale building energy modeling

In recent years, there has been increasing interest in urban-scale building energy modeling (UBEM) because of its ability to simulate city-scale building energy performance to support sustainable development decision-making and urban planning. However, the credibility of UBEMs is often questionable due to a large number of assumptions in the modeling process [229]. Specifically, envelop thermal properties for UBEMs are often assumed using default or reference values. To this end, as found from this review, infrared thermography has been used to reduce the uncertainties in characterizing a building's envelope thermal properties. However, its application remained at the microscale involving determining a single building's thermal properties [169,179]. Therefore, investigations into using infrared technology at an urban scale to inform building thermal performance and reduce UBEM uncertainties would be a promising research direction. More specifically, it will be interesting to investigate the applicability of techniques and technologies from the local scales that can be used to scale up 3D thermal analysis that has been to date limited to the microscale.

6. Conclusion

In this review, several applications of infrared thermography in the built environment were presented at multiple scales. The review summarizes 197 contributions that were selected for their relevance and classified in accordance with several criteria, including the studied area, infrared system, scale, and application. Data analysis was conducted based on the classification and the chronology of contributions to detect the research gaps that could be addressed in the future. Apart from the research gaps or opportunities, the data analysis shows three main tendencies on applications of infrared thermography to explore the built environment at multiple scales.

Firstly, it is observed that the majority of reviewed studies used infrared thermography to evaluate the thermal performance of buildings, or detect their defects. These applications are often performed at the microscale or building-scale, which explains why a considerable portion of reviewed studies was conducted at this scale. However, a non-negligible part of reviewed studies was interested in other applications at the microscale or building-scale, including the analysis of UHI mitigation strategies, the detection of faulty PV panels, and the observation of urban heat fluxes. In the future, more applications of infrared thermography can certainly be found at the microscale or building-scale to understand the energy efficiency of buildings better. One of them could be creating building energy models from thermal images at the microscale or building scales. UBEMs could be generated using infrared thermography at multiple scales by extension of this application.

Secondly, the observation of the UHI effect is the most frequent application of infrared thermography at higher scales than the microscale or building-scale. This result is certainly justified by the extreme emergency to identify the consequences of intense urbanization, particularly during global warming and climate change. However, the magnitude

of the UHI effect alone does not inform the scientific community on the causes of its aggravation nor on strategies to mitigate it. More detailed studies should be conducted on urban heat fluxes, especially at lower scales than the mesoscale, to better understand contributors and mitigators of the UHI effect.

Thirdly, it was pointed out that thermal images have been linked with a few other data sources to explore the built environment at multiple scales. So far, thermal images have essentially been linked with weather data to estimate urban heat fluxes at lower scales than the mesoscale or city-scale. The small interaction between thermal images and other data sources certainly limits the number of applications. In the future, this limitation could be overcome by integrating thermal images into an IoT and a digital twin platform. A linkage of data collected by an IoT and thermal images should better assess the building energy efficiency. If IoT data and thermal images were together included in a digital twin platform with geospatial data, the scientific community and practitioners would have better visualization tools to analyze the operation of a city and strategies to improve its sustainability.

Declaration of competing interest

The authors declare that they have no known competing financial interests or personal relationships that could have appeared to influence the work reported in this paper.

Acknowledgments

This research is supported by the National Research Foundation and Prime Minister's Office of Singapore under its Campus for Research Excellence and Technological Enterprise (CREATE) program. It was funded through a grant to the Berkeley Education Alliance for Research in Singapore (BEARS) for the Singapore-Berkeley Building Efficiency and Sustainability in the Tropics (SinBerBEST) program. BEARS was established by the University of California, Berkeley, as a center for intellectual excellence in research and education in Singapore.

References

- [1] Pelletier F, Bassarsky L, Gu D, Hetog S, Sim Lai M, Sawyer C, Sporenborg T, Zhang G. World urbanization prospects: the 2018 revision. New York: United Nations, Department of Economic and Social Affairs (DESA), Population Division, Population Estimates and Projections Section; 2018.
- [2] IEA. Tracking buildings 2020. 2020, URL: <https://www.iea.org/reports/tracking-buildings-2020>.
- [3] Cheval S, Micu D, Dumitrescu A, Irimescu A, Frighenciu M, Iojă C, Tudose NC, Davidescu S, Antonescu B. Meteorological and ancillary data resources for climate research in urban areas. *Climate* 2020;8(3):37.
- [4] Ngie A, Abutaleb K, Ahmed F, Darwish A, Ahmed M. Assessment of urban heat island using satellite remotely sensed imagery: a review. *South Afr Geogr J* 2014;96(2):198–214.
- [5] Almeida CRd, T. AC, Gonçalves A. Study of the urban heat island (UHI) using remote sensing data/techniques: A systematic review. *Environments* 2021;8(10):105.
- [6] Balaras CA, Argiriou AA. Infrared thermography for building diagnostics. *Energy Build* 2002;34(2):171–83.
- [7] Rakha T, Gorodetsky A. Review of Unmanned Aerial System (UAS) applications in the built environment: Towards automated building inspection procedures using drones. *Autom Constr* 2018;93:252–64.
- [8] Fox M, Coley D, Goodhew S, De Wilde P. Thermography methodologies for detecting energy related building defects. *Renew Sustain Energy Rev* 2014;40:296–310.
- [9] Kyllili A, Fokaides PA, Christou P, Kalogirou SA. Infrared thermography (IRT) applications for building diagnostics: A review. *Appl Energy* 2014;134:531–49.
- [10] Kirimtat A, Krejcar O. A review of infrared thermography for the investigation of building envelopes: Advances and prospects. *Energy Build* 2018;176:390–406.
- [11] Lucchi E. Applications of the infrared thermography in the energy audit of buildings: A review. *Renew Sustain Energy Rev* 2018;82:3077–90.
- [12] Nardi I, Lucchi E, De Rubeis T, Ambrosini D. Quantification of heat energy losses through the building envelope: A state-of-the-art analysis with critical and comprehensive review on infrared thermography. *Build Environ* 2018;146:190–205.
- [13] Herschel W. XIV. Experiments on the refrangibility of the invisible rays of the sun. *Philos Trans R Soc Lond* 1800;(90):284–92.
- [14] Cornell ES. The radiant heat spectrum from Herschel to Melloni.—II. The work of Melloni and his contemporaries. *Ann Sci* 1938;3(4):402–16.
- [15] Ring EFJ. The historical development of temperature measurement in medicine. *Infrared Phys Technol* 2007;49(3):297–301.
- [16] Langley SP. The bolometer and radiant energy. In: *Proceedings of the American academy of arts and sciences*, Vol. 16. JSTOR; 1880, p. 342–58.
- [17] Kalman T. Television apparatus. 1939, US Patent 2, 158, 259.
- [18] Rogalski A. Infrared detectors: an overview. *Infrared Phys Technol* 2002;43(3–5):187–210.
- [19] Gade R, Moeslund TB. Thermal cameras and applications: a survey. *Mach Vis Appl* 2014;25(1):245–62.
- [20] Fokaides PA, Kalogirou SA. Application of infrared thermography for the determination of the overall heat transfer coefficient (U-Value) in building envelopes. *Appl Energy* 2011;88(12):4358–65.
- [21] Asdrubali F, Baldinelli G, Bianchi F. A quantitative methodology to evaluate thermal bridges in buildings. *Appl Energy* 2012;97:365–73.
- [22] Avdelidis NP, Moropoulou A. Emissivity considerations in building thermography. *Energy Build* 2003;35(7):663–7.
- [23] Dătu S, Iboş L, Candau Y, Mattei S. Improvement of building wall surface temperature measurements by infrared thermography. *Infrared Phys Technol* 2005;46(6):451–67.
- [24] Oke TR. Urban environments. In: *The surface climates of Canada*. McGill-Queen's University Press; 1997, p. 303–27.
- [25] Hertwig D, Grimmond S, Hendry MA, Saunders B, Wang Z, Jeoffrion M, Vidale PL, McGuire PC, Bohnenstengel SI, Ward HC, et al. Urban signals in high-resolution weather and climate simulations: role of urban land-surface characterisation. *Theor Appl Climatol* 2020;142(1):701–28.
- [26] Patino JE, Duque JC. A review of regional science applications of satellite remote sensing in urban settings. *Comput Environ Urban Syst* 2013;37:1–17.
- [27] Price JC. The contribution of thermal data in Landsat multispectral classification. *Photogramm Eng Remote Sens* 1981;47(2):229–36.
- [28] Price JC. Estimating surface temperatures from satellite thermal infrared data—A simple formulation for the atmospheric effect. *Remote Sens Environ* 1983;13(4):353–61.
- [29] Vukovich FM. An analysis of the ground temperature and reflectivity pattern about St. Louis, Missouri, using HCMM satellite data. *J Appl Meteorol Climatol* 1983;22(4):560–71.
- [30] Kidder SQ, Wu H-T. A multispectral study of the St. Louis area under snow-covered conditions using NOAA-7 AVHRR data. *Remote Sens Environ* 1987;22(2):159–72.
- [31] Cohen WB, Justice CO. Validating MODIS terrestrial ecology products: linking in situ and satellite measurements. 1999.
- [32] Roth M, Oke TR, Emery WJ. Satellite-derived urban heat islands from three coastal cities and the utilization of such data in urban climatology. *Int J Remote Sens* 1989;10(11):1699–720.
- [33] Carnahan WH, Larson RC. An analysis of an urban heat sink. *Remote Sens Environ* 1990;33(1):65–71.
- [34] Gallo KP, McNab AL, Karl TR, Brown JF, Hood JJ, Tarpley JD. The use of NOAA AVHRR data for assessment of the urban heat island effect. *J Appl Meteorol* 1993;32(5):899–908.
- [35] Lo CP, Quattrochi DA, Luvalle JC. Application of high-resolution thermal infrared remote sensing and GIS to assess the urban heat island effect. *Int J Remote Sens* 1997;18(2):287–304.
- [36] Streutker DR. A remote sensing study of the urban heat island of Houston, Texas. *Int J Remote Sens* 2002;23(13):2595–608.
- [37] Lo CP, Quattrochi DA. Land-use and land-cover change, urban heat island phenomenon, and health implications. *Photogramm Eng Remote Sens* 2003;69(9):1053–63.
- [38] Nichol J. Remote sensing of urban heat islands by day and night. *Photogramm Eng Remote Sens* 2005;71(5):613–21.
- [39] Chen X-L, Zhao H-M, Li P-X, Yin Z-Y. Remote sensing image-based analysis of the relationship between urban heat island and land use/cover changes. *Remote Sens Environ* 2006;104(2):133–46.
- [40] Goldreich Y. Ground and top of canopy layer urban heat island partitioning on an airborne image. *Remote Sens Environ* 2006;104(2):247–55.
- [41] Le-Xiang Q, Hai-Shan C, Chang J. Impacts of land use and cover change on land surface temperature in the Zhujiang Delta. *Pedosphere* 2006;16(6):681–9.
- [42] Yang H, Liu Y. A satellite remote sensing based assessment of urban heat island in Lanzhou city, northwest China. *Int Arch Photogramm Neth: Remote Sens Spat Inf Sci* 2006.
- [43] Wang K, Wang J, Wang P, Sparrow M, Yang J, Chen H. Influences of urbanization on surface characteristics as derived from the moderate-resolution imaging spectroradiometer: A case study for the Beijing metropolitan area. *J Geophys Res: Atmos* 2007;112(D22).
- [44] Li K, Yu Z. Comparative and combinative study of urban heat island in wuhan city with remote sensing and CFD simulation. *Sensors* 2008;8(10):6692–703.
- [45] Wan Z. New refinements and validation of the MODIS land-surface temperature/emissivity products. *Remote Sens Environ* 2008;112(1):59–74.

- [46] Li J-J, Wang X-R, Wang X-J, Ma W-C, Zhang H. Remote sensing evaluation of urban heat island and its spatial pattern of the Shanghai metropolitan area, China. *Ecol Complex* 2009;6(4):413–20.
- [47] Imhoff ML, Zhang P, Wolfe RE, Bounoua L. Remote sensing of the urban heat island effect across biomes in the continental USA. *Remote Sens Environ* 2010;114(3):504–13.
- [48] Bechtel B. Multitemporal landsat data for urban heat island assessment and classification of local climate zones. In: 2011 joint urban remote sensing event. IEEE; 2011, p. 129–32.
- [49] Liu L, Zhang Y. Urban heat island analysis using the Landsat TM data and ASTER data: A case study in Hong Kong. *Remote Sens* 2011;3(7):1535–52.
- [50] Joshi JP, Bhatt B. Estimating temporal land surface temperature using remote sensing: A study of Vadodara urban area, Gujarat. *Int J Geol Earth Environ Sci* 2012;2(1):123–30.
- [51] Rhinane H, Hilali A, Bahi H, Berrada A. Contribution of landsat TM data for the detection of urban heat islands areas case of casablanca. Scientific Research Publishing; 2012.
- [52] Tomlinson CJ, Chapman L, Thornes JE, Baker CJ. Derivation of Birmingham's summer surface urban heat island from MODIS satellite images. *Int J Climatol* 2012;32(2):214–24.
- [53] Lazzarini M, Marpu PR, Ghedira H. Temperature-land cover interactions: The inversion of urban heat island phenomenon in desert city areas. *Remote Sens Environ* 2013;130:136–52.
- [54] Sobrino JA, Oltra-Carrió R, Sòria G, Jiménez-Muñoz JC, Franch B, Hidalgo V, Mattar C, Julien Y, Cuenca J, Romaguera M, et al. Evaluation of the surface urban heat island effect in the city of Madrid by thermal remote sensing. *Int J Remote Sens* 2013;34(9–10):3177–92.
- [55] Ho HC, Knudby A, Sirovyak P, Xu Y, Hodul M, Henderson SB. Mapping maximum urban air temperature on hot summer days. *Remote Sens Environ* 2014;154:38–45.
- [56] Dihkan M, Karsli F, Guneroglu A, Guneroglu N. Evaluation of surface urban heat island (SUHI) effect on coastal zone: The case of Istanbul Megacity. *Ocean Coast Manage* 2015;118:309–16.
- [57] Scarano M, Sobrino JA. On the relationship between the sky view factor and the land surface temperature derived by Landsat-8 images in Bari, Italy. *Int J Remote Sens* 2015;36(19–20):4820–35.
- [58] Coutts AM, Harris RJ, Phan T, Livesley SJ, Williams NSG, Tapper NJ. Thermal infrared remote sensing of urban heat: Hotspots, vegetation, and an assessment of techniques for use in urban planning. *Remote Sens Environ* 2016;186:637–51.
- [59] Kikon N, Singh P, Singh SK, Vyas A. Assessment of urban heat islands (UHI) of Noida City, India using multi-temporal satellite data. *Sustainable Cities Soc* 2016;22:19–28.
- [60] Li X, Li W, Middel A, Harlan SL, Brazel AJ, Turner II BL. Remote sensing of the surface urban heat island and land architecture in Phoenix, Arizona: Combined effects of land composition and configuration and cadastral-demographic-economic factors. *Remote Sens Environ* 2016;174:233–43.
- [61] Scarano M, Mancini F. Assessing the relationship between sky view factor and land surface temperature to the spatial resolution. *Int J Remote Sens* 2017;38(23):6910–29.
- [62] Shirani-Bidabadi N, Nasrabadi T, Faryadi S, Larijani A, Roodposhti MS. Evaluating the spatial distribution and the intensity of urban heat island using remote sensing, case study of Isfahan city in Iran. *Sustainable Cities Soc* 2019;45:686–92.
- [63] Wang W, Liu K, Tang R, Wang S. Remote sensing image-based analysis of the urban heat island effect in shenzhen, China. *Phys Chem Earth A/B/C* 2019;110:168–75.
- [64] Norman JM, Kustas WP, Prueger JH, Diak GR. Surface flux estimation using radiometric temperature: A dual-temperature-difference method to minimize measurement errors. *Water Resour Res* 2000;36(8):2263–74.
- [65] Ma Y, Tsukamoto O, Ishikawa H, Su Z, Menenti M, Wang J, Wen J. Determination of regional land surface heat flux densities over heterogeneous landscape of HEIFE integrating satellite remote sensing with field observations. *J Meteorol Soc Japan II* 2002;80(3):485–501.
- [66] Chrysoulakis N. Estimation of the all-wave net radiation balance in urban environment with the combined use of Terra/ASTER multispectral imagery and in-situ spatial data. *J Geophys Res* 2003;108(D18):4582.
- [67] French AN, Schmugge TJ, Kustas WP, Brubaker KL, Prueger J. Surface energy fluxes over El Reno, Oklahoma, using high-resolution remotely sensed data. *Water Resour Res* 2003;39(6).
- [68] Bisht G, Venturini V, Islam S, Jiang LE. Estimation of the net radiation using MODIS (Moderate Resolution Imaging Spectroradiometer) data for clear sky days. *Remote Sens Environ* 2005;97(1):52–67.
- [69] Kato S, Yamaguchi Y. Analysis of urban heat-island effect using ASTER and ETM+ Data: Separation of anthropogenic heat discharge and natural heat radiation from sensible heat flux. *Remote Sens Environ* 2005;99(1–2):44–54.
- [70] Wang K, Wan Z, Wang P, Sparrow M, Liu J, Zhou X, Haginoya S. Estimation of surface long wave radiation and broadband emissivity using Moderate Resolution Imaging Spectroradiometer (MODIS) land surface temperature/emissivity products. *J Geophys Res: Atmos* 2005;110(D11).
- [71] Kato S, Yamaguchi Y. Estimation of storage heat flux in an urban area using ASTER data. *Remote Sens Environ* 2007;110(1):1–17.
- [72] Tang B, Li Z-L. Estimation of instantaneous net surface longwave radiation from MODIS cloud-free data. *Remote Sens Environ* 2008;112(9):3482–92.
- [73] Xu W, Wooster MJ, Grimmond CSB. Modelling of urban sensible heat flux at multiple spatial scales: A demonstration using airborne hyperspectral imagery of shanghai and a temperature-emissivity separation approach. *Remote Sens Environ* 2008;112(9):3493–510.
- [74] Bisht G, Bras RL. Estimation of net radiation from the MODIS data under all sky conditions: Southern Great Plains case study. *Remote Sens Environ* 2010;114(7):1522–34.
- [75] Liu Y, Shintaro G, Zhuang D, Kuang W. Urban surface heat fluxes infrared remote sensing inversion and their relationship with land use types. *J Geogr Sci* 2012;22(4):699–715.
- [76] Wu H, Zhang X, Liang S, Yang H, Zhou G. Estimation of clear-sky land surface longwave radiation from MODIS data products by merging multiple models. *J Geophys Res: Atmos* 2012;117(D22).
- [77] Weng Q, Hu X, Quattrochi DA, Liu H. Assessing intra-urban surface energy fluxes using remotely sensed ASTER imagery and routine meteorological data: A case study in Indianapolis, USA. *IEEE J Sel Top Appl Earth Obs Remote Sens* 2013;7(10):4046–57.
- [78] Chen S, Hu D. Parameterizing anthropogenic heat flux with an energy-consumption inventory and multi-source remote sensing data. *Remote Sens* 2017;9(11):1165.
- [79] Chrysoulakis N, Grimmond S, Feigenwinter C, Lindberg F, Gastellu-Etchegorry J-P, Marconcini M, Mitraka Z, Stagakis S, Crawford B, Olofson F, et al. Urban energy exchanges monitoring from space. *Sci Rep* 2018;8(1):1–8.
- [80] Qin B, Cao B, Li H, Bian Z, Hu T, Du Y, Yang Y, Xiao Q, Liu Q. Evaluation of six high-spatial resolution clear-sky surface upward longwave radiation estimation methods with MODIS. *Remote Sens* 2020;12(11):1834.
- [81] Rios G, Ramamurthy P. A novel model to estimate sensible heat fluxes in urban areas using satellite-derived data. *Remote Sens Environ* 2022;270:112880.
- [82] Weng Q, Lu D, Schrubring J. Estimation of land surface temperature-vegetation abundance relationship for urban heat island studies. *Remote Sens Environ* 2004;89(4):467–83.
- [83] Lu D, Weng Q. Spectral mixture analysis of ASTER images for examining the relationship between urban thermal features and biophysical descriptors in Indianapolis, Indiana, USA. *Remote Sens Environ* 2006;104(2):157–67.
- [84] He JF, Liu JY, Zhuang DF, Zhang W, Liu ML. Assessing the effect of land use/land cover change on the change of urban heat island intensity. *Theor Appl Climatol* 2007;90(3):217–26.
- [85] Zhou W, Huang G, Cadenasso ML. Does spatial configuration matter? Understanding the effects of land cover pattern on land surface temperature in urban landscapes. *Landscape Urban Plan* 2011;102(1):54–63.
- [86] Xu H, Lin D, Tang F. The impact of impervious surface development on land surface temperature in a subtropical city: Xiamen, China. *Int J Climatol* 2013;33(8):1873–83.
- [87] Guo G, Wu Z, Xiao R, Chen Y, Liu X, Zhang X. Impacts of urban biophysical composition on land surface temperature in urban heat island clusters. *Landscape Urban Plan* 2015;135:1–10.
- [88] Sannigrahi S, Bhatt S, Rahmat S, Uniyal B, Banerjee S, Chakraborti S, Jha S, Lahiri S, Santra K, Bhatt A. Analyzing the role of biophysical compositions in minimizing urban land surface temperature and urban heating. *Urban Clim* 2018;24:803–19.
- [89] Firozjaei MK, Alavipanah SK, Liu H, Sedighi A, Mijani N, Kiavarz M, Weng Q. A PCA-OLS model for assessing the impact of surface biophysical parameters on land surface temperature variations. *Remote Sens* 2019;11(18):2094.
- [90] Ghosh S, Chatterjee ND, Dinda S. Relation between urban biophysical composition and dynamics of land surface temperature in the kolkata metropolitan area: a GIS and statistical based analysis for sustainable planning. *Model Earth Syst Environ* 2019;5(1):307–29.
- [91] Hu Y, Dai Z, Guldmann J-M. Modeling the impact of 2D/3D urban indicators on the urban heat island over different seasons: A boosted regression tree approach. *J Environ Manage* 2020;266:110424.
- [92] Kim J, Lee D-K, Brown RD, Kim S, Kim J-H, Sung S. The effect of extremely low sky view factor on land surface temperatures in urban residential areas. *Sustainable Cities Soc* 2022;103799.
- [93] Eliasson I. Infrared thermography and urban temperature patterns. *Int J Remote Sens* 1992;13(5):869–79.
- [94] Voogt JA, Oke TR. Effects of urban surface geometry on remotely-sensed surface temperature. *Int J Remote Sens* 1998;19(5):895–920.
- [95] Saaroni H, Ben-Dor E, Bitan A, Potchter O. Spatial distribution and microscale characteristics of the urban heat island in Tel-Aviv, Israel. *Landscape Urban Plan* 2000;48(1–2):1–18.
- [96] Lagouarde J-P, Moreau P, Irvine M, Bonnefond J-M, Voogt JA, Solliet F. Airborne experimental measurements of the angular variations in surface temperature over urban areas: case study of Marseille (France). *Remote Sens Environ* 2004;93(4):443–62.
- [97] Leuzinger S, Vogt R, Körner C. Tree surface temperature in an urban environment. *Agricult Forest Meteorol* 2010;150(1):56–62.

- [98] Lagouarde J-P, Commando D, Irvine M, Garrigou D. Atmospheric boundary-layer turbulence induced surface temperature fluctuations. Implications for TIR remote sensing measurements. *Remote Sens Environ* 2013;138:189–98.
- [99] Lagüela S, Díaz L, Roca D, Lorenzo H, et al. Aerial thermography from low-cost UAV for the generation of thermographic digital terrain models. *Opto-Electron Rev* 2015;23(1):78–84.
- [100] Honjo T, Tsunematsu N, Yokoyama H, Yamasaki Y, Umeki K. Analysis of urban surface temperature change using structure-from-motion thermal mosaicing. *Urban Clim* 2017;20:135–47.
- [101] Antoniou N, Montazeri H, Neophytou M, Blocken B. CFD simulation of urban microclimate: Validation using high-resolution field measurements. *Sci Total Environ* 2019;695:133743.
- [102] Fabbri K, Costanzo V. Drone-assisted infrared thermography for calibration of outdoor microclimate simulation models. *Sustainable Cities Soc* 2020;52:101855.
- [103] Adderley C, Christen A, Voogt JA. The effect of radiometer placement and view on inferred directional and hemispheric radiometric temperatures of an urban canopy. *Atmos Meas Tech* 2015;8(7):2699–714.
- [104] Morrison W, Yin T, Laurent N, Guilleux J, Kotthaus S, Gastellu-Etchegorry J-P, Norford L, Grimmond S. Atmospheric and emissivity corrections for ground-based thermography using 3D radiative transfer modelling. *Remote Sens Environ* 2020;237:111524.
- [105] Richters J, Meier F, Scherer D. Analysis of long-wave radiation from urban facets derived from time-sequential thermography (TST) and 3D city model. In: 7th international conference on urban climate, Vol. 29. 2009.
- [106] Sham JFC, Lo TY, Memon SA. Verification and application of continuous surface temperature monitoring technique for investigation of nocturnal sensible heat release characteristics by building fabrics. *Energy Build* 2012;53:108–16.
- [107] Dobler G, Bianco FB, Sharma MS, Karpf A, Baur J, Ghandehari M, Wurtelle JS, Koonin SE. The urban observatory: a multi-modal imaging platform for the study of dynamics in complex urban systems. *Remote Sens* 2021;13:108–16.
- [108] Morrison W, Kotthaus S, Grimmond S. Urban surface temperature observations from ground-based thermography: intra-and inter-facet variability. *Urban Clim* 2021;35:100748.
- [109] Stewart I, Oke TR. Newly developed “thermal climate zones” for defining and measuring urban heat island magnitude in the canopy layer. In: Eighth symposium on urban environment, Phoenix, AZ. 2009.
- [110] Kustas WP, Norman JM. Use of remote sensing for evapotranspiration monitoring over land surfaces. *Hydrol Sci J* 1996;41(4):495–516.
- [111] Carlson TN, Gillies RR, Perry EM. A method to make use of thermal infrared temperature and NDVI measurements to infer surface soil water content and fractional vegetation cover. *Remote Sens Rev* 1994;9(1–2):161–73.
- [112] Gillies RR, Carlson TN. Thermal remote sensing of surface soil water content with partial vegetation cover for incorporation into climate models. *J Appl Meteorol Climatol* 1995;34(4):745–56.
- [113] Krayenhoff ES, Voogt JA. A microscale three-dimensional urban energy balance model for studying surface temperatures. *Bound-Lay Meteorol* 2007;123(3):433–61.
- [114] D’Agostino D, Cuniberti B, Bertoldi P. Energy consumption and efficiency technology measures in European non-residential buildings. *Energy Build* 2017;153:72–86.
- [115] Berardi U. Building energy consumption in US, EU, and BRIC countries. *Procedia Eng* 2015;118:128–36.
- [116] Grinzato E, Vavilov V, Kauppinen T. Quantitative infrared thermography in buildings. *Energy Build* 1998;29(1):1–9.
- [117] Haralambopoulos DA, Paparsenos GF. Assessing the thermal insulation of old buildings - The need for in situ spot measurements of thermal resistance and planar infrared thermography. *Energy Convers Manage* 1998;39(1–2):65–79.
- [118] Li Z, Yao W, Lee S, Lee C, Yang Z. Application of infrared thermography technique in building finish evaluation. *J Nondestruct Eval* 2000;19(1):11–9.
- [119] Grinzato E, Bison PG, Marinetti S. Monitoring of ancient buildings by the thermal method. *J Cult Herit* 2002;3(1):21–9.
- [120] Rosina E, Spodek J, et al. Using infrared thermography to detect moisture in masonry: Case study in Indiana. 2003.
- [121] Ocaña SM, Guerrero IC, Requena IG. Thermographic survey of two rural buildings in Spain. *Energy Build* 2004;36(6):515–23.
- [122] Al-Kassir AR, Fernandez J, Tinaut FV, Castro F. Thermographic study of energetic installations. *Appl Therm Eng* 2005;25(2–3):183–90.
- [123] Meola C, Di Maio R, Roberti N, Carlomagno GM. Application of infrared thermography and geophysical methods for defect detection in architectural structures. *Eng Fail Anal* 2005;12(6):875–92.
- [124] Tavukcuoğlu A, Düzgüneş A, Caner-Saltık EN, Demirci Ş. Use of IR thermography for the assessment of surface-water drainage problems in a historical building, Ağzıkarahan (Aksaray), Turkey. *NDT & E Int* 2005;38(5):402–10.
- [125] Martínez-De Dios JR, Ollero A. Automatic detection of windows thermal heat losses in buildings using UAVs. In: 2006 world automation congress. IEEE; 2006, p. 1–6.
- [126] Meola C. Infrared thermography of masonry structures. *Infrared Phys Technol* 2007;49(3):228–33.
- [127] Ribarić S, Marčetić D, Vedin DS. A knowledge-based system for the non-destructive diagnostics of façade isolation using the information fusion of visual and IR images. *Expert Syst Appl* 2009;36(2):3812–23.
- [128] Vavilov VP. A pessimistic view of the energy auditing of building structures with the use of infrared thermography. *Russ J Nondestruct Test* 2010;46(12):906–10.
- [129] Zalewski L, Lassus S, Rousse D, Boukhalfa K. Experimental and numerical characterization of thermal bridges in prefabricated building walls. *Energy Convers Manage* 2010;51(12):2869–77.
- [130] Grinzato E, Ludwig N, Cadelano G, Bertucci M, Gargano M, Bison P. Infrared thermography for moisture detection: a laboratory study and in-situ test. *Mater Eval* 2011;69(1):97–104.
- [131] Kordatos EZ, Exarchos DA, Stavrakos C, Moropoulou A, Matikas TE. Infrared thermographic inspection of murals and characterization of degradation in historic monuments. *Constr Build Mater* 2013;48:1261–5.
- [132] Cerdeira F, Vázquez ME, Collazo J, Granada E. Applicability of infrared thermography to the study of the behaviour of stone panels as building envelopes. *Energy Build* 2011;43(8):1845–51.
- [133] Lerma JL, Cabrelles M, Portalés C. Multitemporal thermal analysis to detect moisture on a building façade. *Constr Build Mater* 2011;25(5):2190–7.
- [134] Avdelidis NP, Moropoulou A. Applications of infrared thermography for the investigation of historic structures. *J Cult Herit* 2004;5(1):119–27.
- [135] Hopper J, Littlewood JR, Taylor T, Counsell JAM, Thomas AM, Karani G, Geens A, Evans NI. Assessing retrofitted external wall insulation using infrared thermography. *Struct Surv* 2012.
- [136] Paoletti D, Ambrosini D, Sfarra S, Bisegna F. Preventive thermographic diagnosis of historical buildings for consolidation. *J Cult Herit* 2013;14(2):116–21.
- [137] Bianchi F, Pisello AL, Baldinelli G, Asdrubali F. Infrared thermography assessment of thermal bridges in building envelope: Experimental validation in a test room setup. *Sustainability* 2014;6(10):7107–20.
- [138] Edis E, Flores-Colen I, De Brito J. Passive thermographic detection of moisture problems in façades with adhered ceramic cladding. *Constr Build Mater* 2014;51:187–97.
- [139] Lerma C, Mas A, Gil E, Vercher J, Peñalver MJ. Pathology of building materials in historic buildings. Relationship between laboratory testing and infrared thermography. *Mater Constr* 2014;64(313):009.
- [140] Taylor T, Counsell J, Gill S. Combining thermography and computer simulation to identify and assess insulation defects in the construction of building façades. *Energy Build* 2014;76:130–42.
- [141] Edis E, Flores-Colen I, De Brito J. Quasi-quantitative infrared thermographic detection of moisture variation in facades with adhered ceramic cladding using principal component analysis. *Build Environ* 2015;94:97–108.
- [142] Fox M, Coley D, Goodhew S, De Wilde P. Time-lapse thermography for building defect detection. *Energy Build* 2015;92:95–106.
- [143] Lai WW-L, Lee K-K, Poon C-S. Validation of size estimation of debonds in external wall’s composite finishes via passive infrared thermography and a gradient algorithm. *Constr Build Mater* 2015;87:113–24.
- [144] Barreira E, Almeida RMSF, Delgado JMPQ. Infrared thermography for assessing moisture related phenomena in building components. *Constr Build Mater* 2016;110:251–69.
- [145] Fox M, Goodhew S, De Wilde P. Building defect detection: External versus internal thermography. *Build Environ* 2016;105:317–31.
- [146] Barreira E, Almeida RMSF, Moreira M. An infrared thermography passive approach to assess the effect of leakage points in buildings. *Energy Build* 2017;140:224–35.
- [147] Marino BM, Muñoz N, Thomas LP. Estimation of the surface thermal resistances and heat loss by conduction using thermography. *Appl Therm Eng* 2017;114:1213–21.
- [148] O’Grady M, Lechowska AA, Harte AM. Infrared thermography technique as an in-situ method of assessing heat loss through thermal bridging. *Energy Build* 2017;135:20–32.
- [149] Baldinelli G, Bianchi F, Rotili A, Costarelli D, Seracini M, Vinti G, Asdrubali F, Evangelisti L. A model for the improvement of thermal bridges quantitative assessment by infrared thermography. *Appl Energy* 2018;211:854–64.
- [150] Bauer E, Milhomem PM, Aidar LAG. Evaluating the damage degree of cracking in facades using infrared thermography. *J Civ Struct Health Monit* 2018;8(3):517–28.
- [151] Mauriello ML. Designing and evaluating next-generation thermographic systems to support residential energy audits (Ph.D. thesis), College Park: University of Maryland; 2018.
- [152] O’Grady M, Lechowska AA, Harte AM. Application of infrared thermography technique to the thermal assessment of multiple thermal bridges and windows. *Energy Build* 2018;168:347–62.
- [153] Tejedor B, Barreira E, Almeida RMSF, Casals M. Thermographic 2D U-value map for quantifying thermal bridges in building façades. *Energy Build* 2020;224:110176.
- [154] Rakha T, El Masri Y, Chen K, Panagoulia E, De Wilde P. Building envelope anomaly characterization and simulation using drone time-lapse thermography. *Energy Build* 2021;111754.
- [155] Albatici R, Tonelli AM. Infrared thermovision technique for the assessment of thermal transmittance value of opaque building elements on site. *Energy Build* 2010;42(11):2177–83.

- [156] Lagiela S, Martínez J, Armesto J, Arias P. Energy efficiency studies through 3D laser scanning and thermographic technologies. *Energy Build* 2011;43(6):1216–21.
- [157] Lagiela S, Armesto J, Arias P, Herráez J. Automation of thermographic 3D modelling through image fusion and image matching techniques. *Autom Constr* 2012;27:24–31.
- [158] Dall'O G, Sarto L, Panza A, et al. Infrared screening of residential buildings for energy audit purposes: results of a field test. *Energies* 2013;6(8):3859–78.
- [159] González-Aguilera D, Laguela S, Rodríguez-González P, Hernández-López D. Image-based thermographic modeling for assessing energy efficiency of buildings façades. *Energy Build* 2013;65:29–36.
- [160] Ham Y, Golparvar-Fard M. An automated vision-based method for rapid 3D energy performance modeling of existing buildings using thermal and digital imagery. *Adv Eng Inform* 2013;27(3):395–409.
- [161] Lagiela S, Díaz-Vilarino L, Martínez J, Armesto J. Automatic thermographic and RGB texture of as-built BIM for energy rehabilitation purposes. *Autom Constr* 2013;31:230–40.
- [162] Lehmann B, Wakili KG, Frank T, Collado BV, Tanner C. Effects of individual climatic parameters on the infrared thermography of buildings. *Appl Energy* 2013;110:29–43.
- [163] Wang C, Cho YK, Gai M. As-is 3D thermal modeling for existing building envelopes using a hybrid LIDAR system. *J Comput Civ Eng* 2013;27(6):645–56.
- [164] Baldinelli G, Bianchi F. Windows thermal resistance: Infrared thermography aided comparative analysis among finite volumes simulations and experimental methods. *Appl Energy* 2014;136:250–8.
- [165] Lagiela S, Díaz-Vilarino L, Roca D, Armesto J. Aerial oblique thermographic imagery for the generation of building 3D models to complement geographic information systems. In: 12th international conference on quantitative infrared thermography (QIRT 2014), Vol. 10. 2014.
- [166] Lagiela S, Díaz-Vilarino L, Armesto J, Arias P. Non-destructive approach for the generation and thermal characterization of an as-built BIM. *Constr Build Mater* 2014;51:55–61.
- [167] Wakili KG, Binder B, Zimmermann M, Tanner C. Efficiency verification of a combination of high performance and conventional insulation layers in retrofitting a 130-year old building. *Energy Build* 2014;82:237–42.
- [168] Albatici R, Tonelli AM, Chiogna M. A comprehensive experimental approach for the validation of quantitative infrared thermography in the evaluation of building thermal transmittance. *Appl Energy* 2015;141:218–28.
- [169] Ham Y, Golparvar-Fard M. Mapping actual thermal properties to building elements in gbXML-based BIM for reliable building energy performance modeling. *Autom Constr* 2015;49:214–24.
- [170] Nardi I, Ambrosini D, De Rubeis T, Sferra S, Perilli S, Pasqualoni G. A comparison between thermographic and flow-meter methods for the evaluation of thermal transmittance of different wall constructions. In: *Journal of physics: Conference series*, Vol. 655. IOP Publishing; 2015.
- [171] Gaspar K, Casals M, Gangoles M. A comparison of standardized calculation methods for in situ measurements of façades U-value. *Energy Build* 2016;130:592–9.
- [172] Kim J, Lee J, Kim J, Jang C, Jeong H, Song D. Appropriate conditions for determining the temperature difference ratio via infrared camera. *Build Serv Eng Res Technol* 2016;37(3):272–87.
- [173] Choi DS, Ko MJ. Comparison of various analysis methods based on heat flowmeters and infrared thermography measurements for the evaluation of the in situ thermal transmittance of opaque exterior walls. *Energies* 2017;10(7):1019.
- [174] Maroy K, Carbonez K, Steeman M, Van Den Bossche N. Assessing the thermal performance of insulating glass units with infrared thermography: Potential and limitations. *Energy Build* 2017;138:175–92.
- [175] Tejedor B, Casals M, Gangoles M, Roca X. Quantitative internal infrared thermography for determining in-situ thermal behaviour of façades. *Energy Build* 2017;151:187–97.
- [176] Baffa MD. Assessing overall thermal conductance value of low-rise residential home exterior above-grade walls using infrared thermography methods. *Int J Civ Environ Eng* 2018;12(6):626–36.
- [177] Bienvenido-Huertas D, Rodríguez-Álvarez R, Moyano JJ, Rico F, Marín D. Determining the U-value of façades using the thermometric method: Potentials and limitations. *Energies* 2018;11(2):360.
- [178] Gaspar K, Casals M, Gangoles M. In situ measurement of façades with a low U-value: Avoiding deviations. *Energy Build* 2018;170:61–73.
- [179] Marshall A, Francou J, Fitton R, Swan W, Owen J, Benjaber M. Variations in the U-value measurement of a whole dwelling using infrared thermography under controlled conditions. *Buildings* 2018;8(3):46.
- [180] Tejedor B, Casals M, Gangoles M. Assessing the influence of operating conditions and thermophysical properties on the accuracy of in-situ measured U-values using quantitative internal infrared thermography. *Energy Build* 2018;171:64–75.
- [181] Yang M-D, Su T-C, Lin H-Y. Fusion of infrared thermal image and visible image for 3D thermal model reconstruction using smartphone sensors. *Sensors* 2018;18(7):2003.
- [182] Bienvenido-Huertas D, Bermúdez J, Moyano J, Marín D. Comparison of quantitative IRT to estimate U-value using different approximations of ECHTC in multi-leaf walls. *Energy Build* 2019;184:99–113.
- [183] Choi DS, Ko MJ. Analysis of convergence characteristics of average method regulated by ISO 9869-1 for evaluating in situ thermal resistance and thermal transmittance of opaque exterior walls. *Energies* 2019;12(10):1989.
- [184] Gaši M, Milovanović B, Gumbarević S. Comparison of infrared thermography and heat flux method for dynamic thermal transmittance determination. *Buildings* 2019;9(5):132.
- [185] Lu X, Memari A. Application of infrared thermography for in-situ determination of building envelope thermal properties. *J Build Eng* 2019;26:100885.
- [186] Sen A, Al-Habaibeh A. The design of a novel approach for the assessment of thermal insulation in buildings using infrared thermography and artificial intelligence. *Int J Des Eng* 2019;9(1):65–77.
- [187] Tejedor B, Casals M, Macarulla M, Giretti A. U-value time series analyses: Evaluating the feasibility of in-situ short-lasting IRT tests for heavy multi-leaf walls. *Build Environ* 2019;159:106123.
- [188] Sadhukhan D, Peri S, Sugunary N, Biswas A, Selvaraj DF, Koiner K, Rosener A, Dunlevy M, Goveas N, Flynn D, et al. Estimating surface temperature from thermal imagery of buildings for accurate thermal transmittance (U-value): A machine learning perspective. *J Build Eng* 2020;32:101637.
- [189] Tejedor B, Gaspar K, Casals M, Gangoles M. Analysis of the applicability of non-destructive techniques to determine in situ thermal transmittance in passive house façades. *Appl Sci* 2020;10(23):8337.
- [190] Bayomi N, Nagpal S, Rakha T, Fernandez JE. Building envelope modeling calibration using aerial thermography. *Energy Build* 2021;233:110648.
- [191] Mahmoodzadeh M, Gretka V, Hay K, Steele C, Mukhopadhyaya P. Determining overall heat transfer coefficient (U-Value) of wood-framed wall assemblies in Canada using external infrared thermography. *Build Environ* 2021;199:107897.
- [192] Papadakis G, Marinakis V, Konstas C, Doukas H, Papadopoulos A. Managing the uncertainty of the U-value measurement using an auxiliary set along with a thermal camera. *Energy Build* 2021;242:110984.
- [193] Park S, Kim SH, Jeong H, Do SL, Kim J. In situ evaluation of the U-value of a window using the infrared method. *Energies* 2021;14(7):1904.
- [194] Tejedor B, Barreira E, Almeida RMSF, Casals M. Automated data-processing technique: 2D map for identifying the distribution of the U-value in building elements by quantitative internal thermography. *Autom Constr* 2021;122:103478.
- [195] Mastrapostoli E, Santamouris M, Kolokotsa D, Vassilis P, Venieri D, Gompakis K. On the ageing of cool roofs: Measure of the optical degradation, chemical and biological analysis and assessment of the energy impact. *Energy Build* 2016;114:191–9.
- [196] Monteiro CM, Calheiros CSC, Martins JP, Costa FM, Palha P, De Freitas S, Ramos NMM, Castro PML. Substrate influence on aromatic plant growth in extensive green roofs in a Mediterranean climate. *Urban Ecosyst* 2017;20(6):1347–57.
- [197] Chui AC, Gittelsohn A, Sebastian E, Stampler N, Gaffin SR. Urban heat islands and cooler infrastructure—measuring near-surface temperatures with hand-held infrared cameras. *Urban Clim* 2018;24:51–62.
- [198] Kolokotsa D-D, Giannariakis G, Gobakis K, Giannarakis G, Synnefa A, Santamouris M. Cool roofs and cool pavements application in Acharnes, Greece. *Sustainable Cities Soc* 2018;37:466–74.
- [199] Garcia-Nevado E, Beckers B, Coch H. Assessing the cooling effect of urban textile shading devices through time-lapse thermography. *Sustainable Cities Soc* 2020;63:102458.
- [200] Cho Y-I, Yoon D, Shin J, Lee M-J. Comparative analysis of the effects of heat island reduction techniques in Urban Heatwave Areas using drones. *Korean J Remote Sens* 2021;37(6,3):1985–99.
- [201] Lee SW, An KE, Jeon BD, Cho KY, Lee SJ, Seo D. Detecting faulty solar panels based on thermal image processing. In: 2018 IEEE international conference on consumer electronics (ICCE). IEEE; 2018, p. 1–2.
- [202] Ismail H, Chikite R, Bandyopadhyay A, Al Jismi N. Autonomous detection of PV panels using a drone. In: ASME international mechanical engineering congress and exposition, Vol. 59414. American Society of Mechanical Engineers; 2019, V004T05A051.
- [203] Et-taleby A, Boussetta M, Benslimane M. Faults detection for photovoltaic field based on k-means, elbow, and average silhouette techniques through the segmentation of a thermal image. *Int J Photoenergy* 2020;2020.
- [204] Henry C, Poudel S, Lee S-W, Jeong H. Automatic detection system of deteriorated PV modules using drone with thermal camera. *Appl Sci* 2020;10(11):3802.
- [205] Hoyano A, Asano K, Kanamaru T. Analysis of the sensible heat flux from the exterior surface of buildings using time sequential thermography. *Atmos Environ* 1999;33(24–25):3941–51.
- [206] Feng L, Tian H, Qiao Z, Zhao M, Liu Y. Detailed variations in urban surface temperatures exploration based on unmanned aerial vehicle thermography. *IEEE J Sel Top Appl Earth Obs Remote Sens* 2019;13:204–16.

- [207] Arjunan P, Dobler G, Lee K, Miller C, Biljecki F, Poolla K. Operational characteristics of residential air conditioners with temporally granular remote thermographic imaging. In: Proceedings of the 8th ACM international conference on systems for energy-efficient buildings, cities, and transportation. 2021, p. 184–7.
- [208] Gluch R, Quattrochi DA, Luvall JC. A multi-scale approach to urban thermal analysis. *Remote Sens Environ* 2006;104(2):123–32.
- [209] Golden JS, Kaloush KE. Mesoscale and microscale evaluation of surface pavement impacts on the urban heat island effects. *Int J Pavement Eng* 2006;7(1):37–52.
- [210] Hartz DA, Prashad L, Hedquist BC, Golden J, Brazel AJ. Linking satellite images and hand-held infrared thermography to observed neighborhood climate conditions. *Remote Sens Environ* 2006;104(2):190–200.
- [211] Yamazaki F, Murakoshi A, Sekiya N. Observation of urban heat island using airborne thermal sensors. In: 2009 joint urban remote sensing event. IEEE; 2009, p. 1–5.
- [212] Kuo T-H, Liu G-R, Lin T-H, Lan C-W, Huang C-P. A heat island observation via MODIS and concurrent Helicopter-Borne IR imager. *J Mar Sci Technol* 2013;21(6):7.
- [213] Parlow E, Vogt R, Feigenwinter C. The urban heat island of Basel—seen from different perspectives. *DIE ERDE—J Geogr Soc Berlin* 2014;145(1–2):96–110.
- [214] Bonafoni S, Anniballe R, Gioli B, Toscano P. Downscaling landsat land surface temperature over the urban area of Florence. *Eur J Remote Sens* 2016;49(1):553–69.
- [215] Bonafoni S, Tosi G. Downscaling of land surface temperature using airborne high-resolution data: a case study on Aprilia, Italy. *IEEE Geosci Remote Sens Lett* 2016;14(1):107–11.
- [216] Santhanavanich T, Coors V. CityThings: An integration of the dynamic sensor data to the 3D city model. *Environ Plan B* 2021;48(3):417–32. <http://dx.doi.org/10.1177/2399808320983000>.
- [217] Biljecki F, Lim J, Crawford J, Moraru D, Tauscher H, Konde A, Adouane K, Lawrence S, Janssen P, Stouffs R. Extending CityGML for IFC-sourced 3D city models. *Autom Constr* 2021;121:103440. <http://dx.doi.org/10.1016/j.autcon.2020.103440>.
- [218] Chen W, Wu AN, Biljecki F. Classification of urban morphology with deep learning: Application on urban vitality. *Comput Environ Urban Syst* 2021;90:101706. <http://dx.doi.org/10.1016/j.compenvurbsys.2021.101706>.
- [219] Park Y, Guldmann J-M, Liu D. Impacts of tree and building shades on the urban heat island: Combining remote sensing, 3D digital city and spatial regression approaches. *Comput Environ Urban Syst* 2021;88:101655. <http://dx.doi.org/10.1016/j.compenvurbsys.2021.101655>.
- [220] Ledoux H, Arroyo Ohori K, Kumar K, Dukai B, Labetski A, Vitalis S. CityJSON: A compact and easy-to-use encoding of the citygml data model. *Open Geospat Data Softw Stand* 2019;4:4. <http://dx.doi.org/10.1186/s40965-019-0064-0>.
- [221] Ito K, Biljecki F. Assessing bikeability with street view imagery and computer vision. *Transp Res C* 2021;132:103371. <http://dx.doi.org/10.1016/j.trc.2021.103371>.
- [222] Kruse J, Kang Y, Liu Y-N, Zhang F, Gao S. Places for play: Understanding human perception of playability in cities using street view images and deep learning. *Comput Environ Urban Syst* 2021;90:101693. <http://dx.doi.org/10.1016/j.compenvurbsys.2021.101693>.
- [223] Yang J, Rong H, Kang Y, Zhang F, Chegut A. The financial impact of street-level greenery on new york commercial buildings. *Landsc Urban Plan* 2021;214:104162. <http://dx.doi.org/10.1016/j.landurbplan.2021.104162>.
- [224] Biljecki F, Ito K. Street view imagery in urban analytics and GIS: A review. *Landsc Urban Plan* 2021;215:104217. <http://dx.doi.org/10.1016/j.landurbplan.2021.104217>.
- [225] Zhang Y, Cheng T. Graph deep learning model for network-based predictive hotspot mapping of sparse spatio-temporal events. *Comput Environ Urban Syst* 2020;79:101403. <http://dx.doi.org/10.1016/j.compenvurbsys.2019.101403>.
- [226] Wu AN, Biljecki F. Roofpedia: Automatic mapping of green and solar roofs for an open roofscape registry and evaluation of urban sustainability. *Landsc Urban Plan* 2021;214:104167. <http://dx.doi.org/10.1016/j.landurbplan.2021.104167>.
- [227] Ding X, Fan H, Gong J. Towards generating network of bikeways from Mapillary data. *Comput Environ Urban Syst* 2021;88:101632. <http://dx.doi.org/10.1016/j.compenvurbsys.2021.101632>.
- [228] Helbich M, Poppe R, Oberski D, van Emmichoven MZ, Schram R. Can't see the wood for the trees? An assessment of street view- and satellite-derived greenness measures in relation to mental health. *Landsc Urban Plan* 2021;214:104181. <http://dx.doi.org/10.1016/j.landurbplan.2021.104181>.
- [229] Chong A, Gu Y, Jia H. Calibrating building energy simulation models: A review of the basics to guide future work. *Energy Build* 2021;111533. <http://dx.doi.org/10.1016/j.enbuild.2021.111533>.